THE AXIAL-FLOW COMPRESSOR IN THE FREE-MOLECULE RANGE

by

Charles H. Kruger

S.B., Massachusetts Institute of Technology
(1956)

D.I.C., Imperial College of Science and Technology, London
(1957)

Submitted in Partial Fulfillment
of the Requirements for the
Degree of Doctor of Philosophy

at the

Massachusetts Institute of Technology

January, 1960

Signature of Author...................................
Department of Mechanical Engineering

Certified by...
Thesis Supervisor

Accepted by..
Chairman, Departmental Committee on Graduate Students

ABSTRACT

THE AXIAL-FLOW COMPRESSOR IN THE FREE-MOLECULE RANGE

by

Charles H. Kruger

Submitted to the Department of Mechanical Engineering on
January 11, 1960 in partial fulfillment of the require-
ments for the degree of Doctor of Philosophy.

The performance in the free-molecule range of an axial-flow compressor
with flat-plate blades is analyzed theoretically and experimentally. Under
these conditions, when the gas is extremely rarefied, the usual concepts of
continuum gas dynamics are of little value, and the situation is considered
from a molecular point of view. It is shown that the density difference
across the compressor results from the fact that the fraction of those
molecules incident upon the blades which is transmitted through the com-
pressor is greater for molecules incident from the low-density side than
from the high-density side.

Theoretical calculations are made for both single and multiple blade
rows, using the Monte Carlo method. Results indicate that density ratios
per blade row are significantly greater in the free-molecule range than
at aerodynamic conditions. Density ratio is found to increase with in-
creasing blade speed and decreasing blade angle and to decrease linearly
with the upstream volume flow rate. Multiple-blade-row calculations show
that single-row results may be directly combined with reasonable accuracy.

Experimentally, density measurements across a single rotating blade
row give density ratios as high as sixteen to one and show a good agreement
with the theoretical results. Density ratio is found to decrease markedly
with increasing density level in the transition from the free-molecule
range.

Suggestions are made regarding the design of a rarefied-gas compressor
of this type. A comparison of such a compressor with the commonly employed
oil diffusion pumps shows several favorable aspects. The Monte Carlo method
is found to be a useful tool for the solution of problems involving the
dynamics of rarefied gases.

Thesis Supervisor: Professor A. H. Shapiro
Title: Professor of Mechanical Engineering

TABLE OF CONTENTS

b   Blade chord.

G   Number of samples used in the Monte Carlo analysis.

M   Multiplication factor in the multiple-row computer program.

n   Molecular number density.

N   Number of incident molecules per unit area per unit time.

p   Pressure.

P   Probability that molecules incident from the low-density side
           of the compressor will be transmitted through the blades.

Q   Probability that molecules incident from the high-density side
           of the compressor will be transmitted through the blades.

Q'   Used rather than Q when the blade row adjacent to the high-
           pressure gas is stationary.

r   One of a set of uniformly distributed psuedo-random numbers.

R   Universal gas constant divided by the molecular weight of the gas.

s   Blade spacing in the tangential direction.

S   Ratio of the mean mass speed of the gas, relative to the blades,
           to the most probable molecular speed. $S = V/\sqrt{2RT}$.

T   Temperature.

u_t, v_t,   Components of the mean velocities of molecules leaving the
u_r, v_r blades.

U_t, V_t,   Mean mass velocity components for equivalent Maxwellian velocity
U_r, V_r distributions of molecules leaving the blades.

$\mathcal{U}$ Dimensionless molecular speed.

V   Magnitude of the mean mass velocity of the gas relative to the
           blades.

V_B Blade speed.

α Blade angle with the tangential direction.

β Angle which the mean mass velocity of the gas makes with the axial direction.

σ Standard deviation.

Σ General probability that incident molecules will be transmitted through the blades.

The subscripts 1 and 2 refer to the low and high density sides of the compressor, respectively.

Roman numeral subscripts refer to the number of blade rows.

Symbols used exclusively in the Appendices are defined when introduced and are not included in this list.

CHAPTER I

INTRODUCTION

<u>Types of Vacuum Pumps</u>. The methods employed in vacuum technology for the compression of gases are generally different from those used in other branches of engineering. At aerodynamic pressures axial and centrifugal turbocompressors are used to great advantage, whereas until recently they have not been considered for vacuum work. Turbocompressors normally operate at pressure ratios per stage of only about 1.05 to 1.2 for the axial and 1.5 to 2.0 for the centrifugal; to attain the high overall pressure ratio required in vacuum practice, such pressure ratios would require too many stages to be feasible. Vacuum pumps actually used include rotary and reciprocating positive displacement machines, ejectors, molecular drag pumps, cold traps, gettering pumps and diffusion pumps. A description of the commonly employed vacuum pumps may be found in Guthrie and Wakerling[1]* and Dushman[2]. When pressures below about one micron (10^{-3} mm.Hg) are involved, the method of operation is understood from molecular considerations rather than from the application of the usual principles of gas dynamics.

<u>NRC and Pfeiffer Results</u>. Two sets of recent experimental tests indicate that at sufficiently low pressures axial-flow compressors will produce pressure ratios significantly greater than those obtained at aerodynamic pressures. Hablanian[3] at the NRC Equipment Corporation tested a ten-stage axial-flow supercharger at tip speeds of 580 ft./sec. in series with a rotary-piston vacuum pump which discharged to the

---

*Numbers in parenthesis refer to the bibliography.

atmosphere. The machine developed an overall pressure ratio of 70 at an inlet pressure of 3×10^{-4} mm.Hg and no throughflow. In spite of the limitations of these tests--difficulty was experienced eliminating leaks in the forty paper-based gaskets in the compressor housing--a favorable comparison may be made with the overall pressure ratio of 1.7 obtained with this machine at atmospheric inlet and the same tip speed. Measured pressure ratio was found to decrease with increasing pressure and with a net throughflow. As a result of the blade dimensions, the free-molecule range (the region in which the molecular mean-free-path is greater than relevant physical dimensions) was reached by only the inlet stages in the lowest pressure run and not at all in the other runs.

In addition to the above results, the German firm of Arthur Pfeiffer GmbH, Wetzlar, has developed a commercial axial-flow vacuum compressor[4,5]. This compressor operates at pressure levels for which oil diffusion pumps are normally employed and, with nineteen stages of flat-plate blades and tip speeds of about 475 ft./sec., is said to attain pressure ratios as high as 5×10^{7}, and an ultimate vacuum better than 10^{-9} mm. Hg. At only the lowest pressure levels (highest pressure ratios) does it appear that all stages are in the free-molecule range. An analysis of the data, performed by Mr. Y. Wu, indicates that pressure ratio per stage decreases markedly with increasing pressure in the transition from the free-molecule range. Little information is available concerning the design and theoretical considerations upon which the Pfeiffer pump is based. The description of operation given in the patent[4] and in Vakuum-Technik[5] is at best sketchy and seems to indicate that no thorough analysis of the physical process has been made.

Previous Theoretical Work. Calculations have been made for two special cases of a single row of moving flat-plate blades in the free-molecule range. Finol[6] analyzed the problem of very-widely-spaced blades. In this case the molecular interactions with a given blade are independent of those with other blades, and the airfoil theory of Sanger[7], Tsien[8], and Ashley[9] is applicable in a momentum analysis. Finol's results support the possibility of high pressure ratios in the free-molecule range, although his primary assumption (widely-spaced blades) limits his values to conservative ones when compared with a realistic compressor design.

Professor A. H. Shapiro and the author have performed calculations for the case of very high blade speed compared with the mean molecular speed and zero net throughflow. The assumption of high blade speed allowed the thermal components of velocity of the molecules striking the blades to be neglected. An approximate method was used to account for the multiple molecular reflections within the blades. The results then are not exact even for the case assumed (in particular; the values for blade angle $\alpha = 10°$ are questionable). However, as shown in Figure 2, they again support the possibility of high pressure ratios and give an indication of the importance of blade angle and blade spacing-to-chord ratio.

Objectives of this Investigation. The above experimental and theoretical results indicate that axial-flow compressors may prove useful as rarefied-gas compressors, particularly in the free-molecule range. This investigation is designed to provede a basic understanding of the method of operation of such compressors and to provide

quantitative information regarding their performance. Analyses of both single blade rows and multiple-row compressors are made. The study is limited to the free-molecule range, which seems most promising and offers theoretical simplifications, and to flat-plate blades which again offer simplifications, both in analysis and in manufacture.

In addition to its direct application to rarefied-gas compressors, this investigation illustrates the advantages of the Monte Carlo method in the theoretical analysis of problems related to the molecular flow of gases.

CHAPTER II

BASIC CONCEPTS REGARDING THE OPERATION OF THE COMPRESSOR

Comparison of Fluid and Rarefied-Gas Compressors. The physical
process involved and methods of analysis for compressors operating in a
molecular flow are quite different from those of the usual fluid com-
pressor. The main limitations upon pressure ratio, including those
usually associated with decreasing Reynolds numbers,--adverse pressure
gradients, separation, shock waves, surging, and stalling--are no
longer relevant. Efficiency loses its usual significance, since at low
densities the power absorbed by the gas is in any case small. The
fundamental assumptions of continuum analysis cease to hold and the
process must be understood from a molecular point of view.

Free-Molecule Flow. The free-molecule range of gas dynamics is
defined as that regime of densities in which collisions between molecules
are relatively improbable when compared with collisions between molecules
and the boundaries of the gas. For intermolecular collisions to be
improbable within a blade row, the molecular mean-free-path must be
sufficiently large in comparison with the blade dimensions. Tsien[8]
defines the free-molecule range as that condition for which the Knudson
number (the ratio of mean-free-path to a relevant length) is greater
than ten. For comparison, the mean-free-path in air at 20°C is
$\frac{4.86}{p}$ cm., where p is the pressure in microns (10^{-3} mm. Hg)[1].

Method of Operation of the Compressor. An axial-flow compressor
operating in the free-molecule range establishes a density difference by
acting as a barrier of different permeability to the molecules incident
from its high and low density sides. Molecules incident upon the com-
pressor from the low density side have a greater probability of being

transmitted through the blades than molecules incident from the high density side.

Consider a single blade row moving in rarefied gas for which there is no net throughflow from one side of the blades to the other. If P_I is the probability that a molecule incident upon the blades from upstream will be transmitted through the blades to the other side (after, most likely, a series of collisions with the blades) and Q_I is the similar probability of transmission from downstream where $P_I > Q_I$, and if N_1 and N_2 are the number of molecules incident upon the blade row per second per area from upstream and downstream, the condition of zero net throughflow is

$$N_1 \, P_I = N_2 \, P_I \; . \qquad\qquad 2.1$$

If N_1 and N_2 are proportional to n_1 and n_2 , the upstream and downstream number densities, respectively,

$$\frac{n_2}{n_1} \;=\; \frac{P_I}{Q_I} \;>\; 1 \; . \qquad\qquad 2.2$$

Equation 2.2 holds as well for a multiple-row compressor if P_I and Q_I are replaced by overall transmission probabilities.

The extension to the case of a net throughflow will be discussed later. The main point remains the same: the density difference across an axial-flow compressor operating in the free-molecule range is set up by means of the difference between the probabilities of molecular transmission from upstream and downstream. The essential analytical problem lies in the computation of these probabilities.

Two observations may be made immediately. The first is that the blade geometry should be such that a relatively large fraction of the molecules incident from one side are transmitted through the blades, while molecules from the other side are largely reflected away from the blades. Favorable blade designs may then be determined for the most part from a geometrical point of view. Secondly, since intermolecular collisions are improbable in the region between the blades, individual molecules or groups of molecules may be considered separately. This makes possible several simplifications in the analysis. For example, molecules originally incident upon one side of a blade row are transmitted through or reflected from the blades independently and are not affected by those molecules incident from the other direction.

CHAPTER III

THE PHYSICAL MODEL AND ANALYTICAL PROBLEM FOR A SINGLE BLADE ROW

<u>Idealizations and Assumptions</u>. The model adopted in the case of a

single blade row consists of a geometrically two-dimensional row of

flat-plate blades moving between two regions of a three-dimensional

gas. That is, the blade height is large compared to chord and spacing

and the blade shape is two-dimensional and does not change in the

direction of blade height, while the gas molecules move with three-

dimensional velocity components. The gas molecules in the regions on

either side of the blade row are assumed to be moving with Maxwellian

velocity distributions around mean mass velocities relative to the

blades. The molecular mean-free-path is assumed to be large compared

with all blade dimensions but small when compared with any of the

dimensions of the gas regions[*]. Thus molecules reflected or transmitted

from the blades have little chance of colliding with molecules approach-

ing the blades, maintaining the Maxwellian distribution of incident

molecules. This model is illustrated in Figure 1, where α is the

blade angle with the axial direction, s/b the spacing-to-chord ratio,

V_1 and V_2 the magnitudes of the mean mass velocities relative to the

blades upstream and downstream, β_1 and β_2 the angles of these

velocities with the axial direction, and S_1 and S_2 the ratios of

V_1 and V_2 to the most probable molecular speed, $\sqrt{2RT}$ [**].

---

[*]   The flow will be free-molecular as long as the mean-free-path is
large when compared to any of the blade dimensions. This hypothetical
model requires it to be longer than all blade dimensions to maintain
the Maxwellian distribution of incident molecules.

[**] $\sqrt{2RT}$ = 1350 ft/sec for air at 20°C.

Thus,

$$S_1 = V_1/ \sqrt{2RT_1}$$
$$S_2 = V_2/ \sqrt{2RT_2} .$$

3.1

V_1 and V_2 are assumed to have components only in the axial and tangential directions and, since they are relative velocities, account for the blade velocity.

The model is, of course, somewhat unrealistic geometrically. However, calculations based upon it should have a much broader significance. The restriction of large blade height compared with spacing and chord is the usual one made to neglect the effect of the end walls of the flow passage between the blades. This is likely to hold true to a great extent in actual machines, since blades of small chord would be convenient from a design standpoint and would lessen axial drag and since large blade heights would give greater flow areas in which to capture incident molecules.

The assumption of conditions necessary to obtain a Maxwellian velocity distribution for molecules incident upon the blades presents more serious difficulties. The velocity distribution of molecules incident upon a blade row, whether from a region upstream or downstream or from other blades in a multiple-row compressor, will in general be other than Maxwellian, depending on exact conditions and geometry involved. However, since the Maxwellian distribution contains all the important characteristics of the molecular motion, it is not uncommon in kinetic theory to use this distribution or results obtained from it in non-equilibrium situations; see, for example, Kennard[10] or Mott-Smith[11]. With regard to the single blade row it would be

possible in principle to account for deviations from the Maxwellian distribution consistent with any given shape of flow passage, such as annular regions upstream and downstream of the blades. Not only would this be quite involved, but it would be of limited value, since the single blade row results are important mainly as they can be combined in multiple-row calculations. Because of this, further discussion of this part of the model will be left to the sections dealing with those calculations.

Two remaining assumptions are required to complete the picture. The first is that the process is essentially isothermal. This follows from the fact that, at the low densities involved, the energy transferred to the blades and housing by molecular collisions is small compared with the rate at which energy may be conducted or radiated away. Thus, the blades, the housing, and the gas will be at a uniform temperature. The final assumption regards the nature of the molecular collisions with the blades. Although the mechanism of molecule-surface interaction is imperfectly understood, experimental studies[12, 13] indicate that molecules actually leave the surface in an approximately diffuse manner. That is, it is assumed that re-emitted molecules have a Maxwellian motion as if they came from behind the surface from an imaginary gas at rest with respect to the surface[14]. Thus, the direction of re-emission is independent of the direction of incidence and all incoming tangential momentum is lost to the surface. From this it can be shown[10] that the fraction of molecules re-emitted from a point on the surface within the solid angle $d\omega$ is proportional to $\cos\theta\,d\omega$, where θ is the angle $d\omega$ makes with the normal to the

surface. This is the usual form of the cosine law of molecular re-emission. With the geometry of the present problem, the two-dimensional form of this relation (derived in Appendix A) states that the fraction of molecules re-emitted within the plane angle $d\theta$ is proportional to $\cos\theta\, d\theta$, where θ is now the angle between $d\theta$ and the normal to the surface.

The Analytical Problem. Since we are concerned with a situation in which the action of individual molecules or groups of molecules may be considered separately, the problem then resolves into one of determining the (ultimate) fate of molecules coming from the left in Figure 1 for various values of the independent variables; the fate of molecules coming from the right is a solution to the same problem with different values of the independent variables. For example, consider a single blade row moving with a speed V_B between two regions of gas at rest. Then relative to the blades

$$V_1 = V_B$$
$$\beta_1 = \pi/2$$
$$V_2 = V_B \tag{3.2}$$
$$\beta_2 = -\pi/2 \;.$$

The density ratio may be found if the probability of molecular transmission is known for the two sets of variables α, s/b, $V_B/\sqrt{2RT}$, $\beta = \pi/2$ and α, s/b, $V_B/\sqrt{2RT}$, $\beta = -\pi/2$.

In general, to calculate density ratios across single blade rows in free-molecule flow, it is necessary to know Σ_I, the probability that a molecule incident upon the blade row from one side will be

transmitted through the blades to the other side, as a function of α, s/b , $S = V/\sqrt{2RT}$, and β . The subscripts on the independent variables are dropped in the general case and, to avoid ambiguity, Σ_I is used for the general probability of transmission, while the special symbols P_I and Q_I refer to this probability for molecules coming from the low and high density sides, respectively (the Roman numeral subscript refers to the number of blade rows). It should also be noted that, in the free-molecule range, the absolute density level and Knudson number are no longer variables.

If W is defined as the ratio of net throughflow in molecules per unit time per unit area to N_1 , the rate of incidence of molecules upon the blades from the left, and conditions do not vary with time (as is assumed throughout this investigation), a mass balance across the blade row gives

$$N_1 \ W = N_1 \ P_I \ - \ N_2 \ Q_I \qquad\qquad 3.3$$

or

$$\frac{N_2}{N_1} = \frac{P_I}{Q_I} - \frac{W}{Q_I} \ . \qquad\qquad 3.4$$

It can easily be shown that, if the molecules incident upon the blade row have a Maxwellian velocity distribution (see Ashley[9])

$$N = \frac{n \ \sqrt{2RT}}{2} \left\{ \frac{1}{\sqrt{\pi}} \ e^{- \ S^2 \ \cos^2} \ + \ S \ \cos\beta \ \left[1 + \operatorname{erf}(S \ \cos\beta \ ) \right] \right\} \qquad 3.5$$

where the error function is defined by

$$\operatorname{erf}(x) = \frac{2}{\sqrt{\pi}} \int_0^x e^{- \ \xi^2} \ d\xi \qquad\qquad 3.6$$

and is tabulated in Tahnke and Emde[15]. A solution to 3.4 using 3.5

gives density ratio as a function of net throughflow. If β_1 and

$\beta_2 = \pm \; \pi/2$,

$$N = \frac{n \sqrt{2RT}}{2 \sqrt{\pi}}$$

3.7

and

$$\frac{n_2}{n_1} = \frac{P_I}{Q_I} - \frac{W}{Q_I} .$$

3.8

W is proportional to the upstream volume flow rate for a given gas and temperature and represents the ratio of the actual flow rate to the maximum possible*. It is called the H_O coefficient when applied to diffusion pumps. (A value of 0.33 is very good for large pumps. Small pumps sometimes have slightly higher coefficients[1].)

The final step in the formulation of the problem is to decide what information will allow the single blade row results to be combined in multiple-row calculations. Since in a multiple-row machine the molecules incident upon a blade row come from the previous row, it is necessary to have some knowledge of the velocities of molecules leaving the blades in the single row calculations. Clearly the best information would give details of the velocity distributions of the leaving molecules. However, this would not only greatly complicate desired results, but would mean that S and β would no longer be sufficient to specify the conditions of incident molecules and would require additional independent variables. The best solution seems to be the computation of the mean velocities of the molecules leaving the blades and the determination of the mean mass velocities of equivalent Maxwellian velocity

---

*Volume flow rate per unit area = $2.29 \times 10^4 W \; \frac{cfm}{ft^2}$ for air at 20°C and $\beta = \pm \; \pi/2$.

distributions which would produce the same mean leaving velocities. Thus, two equivalent Maxwellian distributions--one for the transmitted and one for the reflected molecules--specified by mean mass velocity components can be found which would give the same mean velocities crossing the exit and entrance planes as the actual transmitted and reflected molecules.

In summary then, the problem consists of finding, for molecules originally incident from one side of the blade row, $\sum_I$ and the four mean velocity components relative to the blades of the transmitted and reflected molecules as functions of α, s/b, S, and β.

CHAPTER IV

METHODS OF SOLUTION

<u>Integral Equation and Related Approaches</u>. Any analytical approach
to the problem must account for the multiple molecular collisions with
the blades. In fact, if the number of molecular collisions per second
per area were known at each point on the surface of the blades, it
would be a relatively easy matter to integrate along the blades using
the cosine re-emission law to determine the number of molecules per
second transmitted through the row by each blade. This divided by the
number of incident molecules per second per blade would give the proba-
bility of transmission, $\sum_I$. The mean velocities of the transmitted
and reflected molecules could be determined by similar integrations.

If the rate at which molecules strike a particular point on a blade
is summed over all such molecules coming from the opposite blade surface
and from outside the blade row and the result combined with a similar
equation for a point on the opposite blade surface, an integral equation
is obtained. This equation is given in Appendix B and is a Fredholm
integral equation of the second kind[16]. The kernel is an elliptic
integral of the first kind[17].

The functions involved in the equation are of such a nature that a
closed form solution is not possible. An approach often employed with
integral equations of this type is iteration; the solution can then be
expressed in terms of an infinite series, such as the Neumann series[16].
In fact, successive approximations of this sort can be shown to be
equivalent to accounting for increasing numbers of reflections within
the blades by incident molecules. Experience gained from the Monte Carlo

solution with typical geometries indicates the average molecule striking the blades makes a number of such collisions before being reflected or transmitted. Because of this, a solution using numerical integration, even with the aid of a high-speed digital computer, would require a practically prohibitive amount of computer time for a representative number of values of the independent variables. Further comment on solutions related to the integral equation approach is given in Appendix B.

Monte Carlo Method. Because of the difficulties involved in obtaining numerical solutions by usual mathematical means, the analysis which was performed employed the so-called Monte Carlo method[18,19]. Although this approach is best understood by considering particular examples, it can be said in general that the Monte Carlo method is a sampling method in which a large number of individual cases (samples) of a given situation are considered separately such that various alternatives are selected according to their probability of occurrence. An average over a finite number of samples serves as an approximation to the dependent variable(s) and an estimate can be made of the probability that the error falls within given limits. The selection process is accomplished by some random means of determining which of the alternatives occur--thus the name, Monte Carlo.

Although the method is used as a purely mathematical technique, e.g., for the solution of Laplace's equation, it seems most suitably employed in those situations, such as the neutron diffusion problem, where the sampling process has physical significance. In such cases, the "governing" mathematical formulation, often an integral equation,

may be dispensed with entirely and the solution proceeds directly from

physical reasoning.   This applies as well to the present problem.

CHAPTER V

THE MONTE CARLO METHOD APPLIED TO A SINGLE BLADE ROW

Outline of Single-Blade-Row Calculations. In the free-molecule
compressor problem, the samples in the Monte Carlo method are individual
molecules incident upon the blade row. The fate of the molecule as to
whether it is transmitted through the blades or reflected back and its
velocity components upon leaving the blades are recorded. An average
over a large number of molecules of the fraction transmitted through
the blades gives the probability of transmission, Σ_T. Enough
samples must be used so that averages are (almost) independent of the
number of samples.

The crux of the method consists of allowing the samples to follow
a course dictated by the proper probabilities. This is done in a number
of ways--mechanical "roulette wheels", random number tables[20],
mathematical and electronic pseudo-random number generators, etc. In
this case, the calculations were made on the I.B.M. 704 digital computer
at the M.I.T. Computation Center and pseudo-random numbers uniformly
distributed between zero and one were obtained from the SHARE subroutine
BA N203, using the method of congruences[21]. The nth random number,
r_n , is given by

$$r_n = k^n r_o \pmod{m} \qquad 5.1$$

where k = 991

x_o = 321,528,735

$m = 2^{31} - 1$.

(mod m) indicates the remainder after division by m . Random numbers
of this sort, produced by a recurrence formula, are commonly used and
meet certain statistical tests.

Details of the calculations for a single blade row are given in Appendix C. To illustrate the reasoning involved a brief example is given here:

To determine the angle at which a molecule is re-emitted from a blade surface, use is made of the cosine law of re-emission and uniformly distributed random numbers. Since the number of molecules leaving the surface within the angle θ and $\theta + d\theta$, where θ is measured from the normal to the surface, is proportional to $\cos \theta \, d\theta$, the fraction between θ and $\theta + d\theta$ is $1/2 \cos \theta \, d\theta$; the integral of this quantity between $-\pi/2$ and $\pi/2$ is unity. The angle θ is then selected according to this probability relation by setting

$$r = \int_{-\pi/2}^{\theta} \frac{1}{2} \cos \theta \, d\theta \qquad 5.2$$

where r is one of a set of random numbers uniformly distributed between zero and one. Solving for θ

$$\theta = \sin^{-1} (2r - 1). \qquad 5.3$$

Using similar integrations of the other probability functions, the course of the molecule between the blades is obtained and its ultimate fate determined.

By performing the computations on a high-speed digital computer, a large number of samples may be used for each set of values of the independent variables, giving reasonable accuracy without using excessive machine time. Numerical averages of the five dependent variables (Σ_T, and the leaving velocity components) for 1000 samples require approximately 12 seconds.

Accuracy. For a given number of samples a quantitative estimate may be made of the error in Σ_I by statistical means if a normal curve of error is assumed. Since whether or not a molecule is transmitted through the blade row is similar to any other process which has only two alternatives and a definite probability of occurrence, established methods may be directly applied. If G is the number of samples over which the average is taken, the standard deviation σ is given by

$$\sigma = \sqrt{G\,\Sigma_I(1 - \Sigma_I)}\ . \qquad\qquad 5.4$$

The probability of occurrence of a deviation from the mean greater or equal to various multiples of σ is tabulated[22]. For example, the probability of occurrence of a deviation greater or equal to $1.6\,\sigma$ is 10.96%.

It can be seen that, since the per cent deviation is inversely proportional to $\sqrt{G}$, great accuracy can be obtained only with quite a large number of samples, particularly for small values of Σ_I or $1 - \Sigma_I$. This limits practical calculations over a range of values of the independent variables to an accuracy somewhat less than that normally expected in numerical computation. The process has the advantage, however, that additional groups of samples may be calculated in a particular situation and the results averaged with initial values.

Except where noted to the contrary the results given will be obtained with a sufficient number of samples that the probability of occurrence of an error of 10% or greater is less than 10.96%.

The probability of error in density ratio may be obtained from the probabilities of error of the values of P_I and Q_I used for the calculation. For example, logarithmic differentiation of equation 3.8 at

zero flow shows that the percentage error in density ratio is equal to the difference between the percentage error in P_I and the percentage error in Q_I .

In addition to the above examination of the accuracy of the method, the computer calculations were checked for a particular case against a solution done manually with the aid of a random number table and the equations themselves were given an independent check by Mr. Yau Wu.

Results. For single row comparisons computer calculations were made for various values of s/b, α , and S with $\beta = \pm \; \pi/2$ including all the combinations of the following values:

$$s/b = 0.5, \; 1.0, \; 1.5$$
$$\alpha = 10°, \; 20°, \; 30°, \; 40°$$
$$S = 0.5, \; 1.0, \; 2.0, \; 5.0$$
$$\beta = \pm \; \pi/2 \; .$$

The results obtained apply to a blade row moving through a gas at rest so that S is the blade speed divided by $\sqrt{2RT}$.

Values of Σ_I are tabulated in Appendix D and shown in Figure 3. It is expected that multiple-row design calculations will be made with single-row values of Σ_I and the multiple-row Monte Carlo results. For this reason values of mean velocity components of molecules leaving a single row are not tabulated or shown graphically. Results of the equivalent Maxwellian velocity distribution analysis are given in Chapter VI to support the approximation of Maxwellian velocity distributions.

Using the values of Σ_I with equation 3.8, density ratio at zero flow, flow parameter W at density ratio of unity, and density

ratio vs. flow rate are given as functions of the independent variables is Figures 4 through 10. Since the process is isothermal, pressure ratio and density ratio are equal.

These results indicate in general that zero throughflow density ratios are larger for larger values of S and smaller values of and, to some extent, s/b , with some exceptions. Conversely, the slope of the characteristic curve of n_2/n_1 vs. W generally increases (becomes less favorable) with larger values of S and smaller values of $\propto$ and s/b . Zero throughflow density ratios are a maximum at an optimum (large) value of S for any particular values of $\propto$ and $s/b*$ and decrease asymptoticly to values which compare reasonably well with the infinite blade speed analysis, Figure 2, considering the approximations used in that analysis.

The calculated density ratios are significantly greater than those obtained per blade row from axial-flow compressors operating in the aerodynamic range, particularly for large values of S and small blade angles, $\propto$. The capacity of the compressor to capture incident molecules is at least comparable to that of oil diffusion pumps.

---

*This maximum would occur for $S > 5.0$ with some of the values of $\propto$ and s/b used.

CHAPTER VI

MULTIPLE-STAGE COMPRESSORS

Combination of Single-Blade-Row Results. The most direct calculation of the overall transmission probabilities of a multiple-stage compressor is obtained by treating each blade row in the compressor as if it had the same transmission probabilities as an isolated row. That is, the velocity distribution of molecules leaving a blade row is taken to be Maxwellian with zero mass velocity relative to the blades. For example, consider a multiple-stage compressor for which all rows are geometrically similar and all rotating rows have the same blade speed. With the exception of stationary rows at either end of the compressor, each blade row--rotating or stationary--will have independently the transmission probabilities of a single rotating row, making a contribution to the overall density ratio at zero flow equal to the single row zero flow density ratio.

Once the transmission probabilities for the individual rows are assumed, the overall probabilities are calculated by taking into account all possible multiple reflections between blade rows. The following results will be given for the case where all blade rows are geometrically similar and rotating blades move at the same speed. However, equivalent relations may easily be obtained, in closed form, for any combination of blade geometries.

P_n is defined as the overall transmission probability for molecules incident upon a rotating blade row from the low-density side of a compressor with n blade rows, Q_n is similarly defined for molecules incident from the high-pressure side, and Q'_n is used rather than Q_n

when the blade row adjacent to the high-density gas is stationary. Since a stationary blade row on the low-density side (inlet guide vane) reflects a large fraction of the incident molecules and adds relatively little to the overall density ratio, it will not be considered here.

For two rows,

$$P_{II} = P_I^2 \left[1 + (1-P_I)(1-Q_I) + (1-P_I)^2(1-Q_I)^2 + - - - \right]. \qquad 6.1$$

Using the binomial series,

$$P_{II} = \frac{P_I^2}{1-(1-P_I)(1-Q_I)} . \qquad 6.2$$

Similarly,

$$Q'_{II} = \frac{Q'_I Q_I}{1-(1-P_I)(1-Q_I)} . \qquad 6.3$$

This may be extended to any number of rows with the result that

$$P_n = \frac{P_{n-1} P_I}{1-(1-Q_{n-1})(1-P_I)} \qquad 6.4$$

$$Q_n = \frac{Q_I \, Q_{n-1}}{1-(1-Q_{n-1})(1-P_I)} \qquad 6.5$$

$$Q'_n = \frac{Q'_I Q_{n-1}}{1-(1-Q_{n-1})(1-P_I)} . \qquad 6.6$$

Density ratio as a function of throughflow is obtained by the appropriate modification of equations 3.4 and 3.8

$$\left(\frac{N_2}{N_1}\right)_n = \frac{P_n}{Q_n} - \frac{W}{Q_n}$$

<div align="right">6.7</div>

or

$$\left(\frac{N_2}{N_1}\right)_n = \frac{P_n}{Q'_n} - \frac{W}{Q'_n}$$

where N is given by 3.5. Again if β_1 and $\beta_2 = \pm \pi/2$ or if $S_2 = 0$ and $\beta_1 = + \pi/2$

$$\left(\frac{n_2}{n_1}\right)_n = \frac{P_n}{Q_n} - \frac{W}{Q_n}$$

or

$$\left(\frac{n_2}{n_1}\right)_n = \frac{P_n}{Q'_n} - \frac{W}{Q'_n} \, .$$

<div align="right">6.8</div>

With zero throughflow this becomes, for an odd number of blade rows

$$\left(\frac{n_2}{n_1}\right)_n = \left(\frac{P_I}{Q_I}\right)^n = \left[\left(\frac{n_2}{n_1}\right)_I\right]^n$$

<div align="right">6.9</div>

and for an even number of rows

$$\left(\frac{n_2}{n_1}\right)_n = \left(\frac{P_I}{Q_I}\right)^{n-1} \frac{P_I}{Q'_I} \, .$$

<div align="right">6.10</div>

These results are for blades of negligible tangential thickness. To account for the fraction of the molecules incident upon one row from another that are reflected back due to finite blade thickness, the probabilities P_I, Q_I, and Q'_I in the above equations must be modified. If f is the fraction of the flow area blocked by the blades

and P_I , Q_I , and Q'_I are the appropriate probabilities for a single row with zero blade thickness, the modified probabilities will be

$$P_I{}^* = (1-f)\ P_I$$

$$Q_I{}^* = (1-f)\ Q_I \qquad\qquad 6.11$$

$$Q'_I{}^* = (1-f)\ R_I \ ,$$

Equations 6.4, 6.5, 6.6, 6.7, and 6.8 still hold, using now the modified probabilities of 6.11. By expanding 6.4, 6.5, and 6.6 using 6.11, it can be seen that the equations for density ratio at zero throughflow, 6.9 and 6.10, are unchanged. On the other hand, the slope of the density ratio vs. flow rate characteristic (6.7, 6.8) is adversely affected by increasing values of f , as would be expected.

Application of Equivalent Maxwellian Velocity Distributions between Rows. As outlined in Chapter III, an improvement over the calculations of the previous section may be made if information is available concerning the velocities of the molecules passing from one blade row to another. Due to the complexity of the problem, this information must be in terms of some type of average; average velocity components of the molecules leaving a blade row were selected as being most suitable. These components u_t, v_t, u_r, and v_r can then be related to the mean mass velocity components U_t, V_t, U_r, and V_r of equivalent Maxwellian velocity distributions which would give the same mean velocity components of leaving molecules.

Then, for example, if U_t and V_t are known for the transmitted molecules leaving a blade row moving at a blade speed ratio $\pm S'$ relative to the next row, where U_t and V_t are nondimensionalized

with respect to $\sqrt{2RT}$, the transmitted molecules are considered to have a Maxwellian velocity distribution specified by U_t and $\pm (V_t \pm S')$ relative to the next row. The signs in $\pm (V_t \pm S')$ are determined by the direction of the relative velocities. The calculation for the next row then makes use of the appropriate single-row result, using

$$\beta = \pm \tan^{-1} \frac{V_t \pm S'}{V_t} \quad \text{and} \quad S = \sqrt{U_t^2 + (V_t \pm S')^2} \ .$$

Finite blade thickness may be accounted for by noting that a fraction of incident molecules equal to the fraction of the flow area blocked by the blades is reflected away from each blade row. Assuming diffuse reflection, the Maxwellian mass velocity of these molecules is that of the blade surface from which they are reflected.

In this way, the computation of overall transmission coefficients of a multiple-stage compressor proceeds step by step using the single row results. Since there are a great many possibilities of multiple reflections between blade rows these calculations cannot be reduced to closed forms, as were the results of the previous section, and must be done numerically. They consequently require a considerable effort if more than a few blade rows are involved.

A simplification is afforded by the fact that the single row results give values of u_t and u_r such that U_t and U_r are, in most cases, small when compared with S . The variation in transmission probability with the axial component of mean mass velocity is such that, for the calculations performed here, U_t and U_r may be set equal to zero with little loss in accuracy. This approximation reduces the effective number of independent variables to three (s/b, α, and S).

Multiple-Stage Monte Carlo Solution. Both methods previously described in this chapter have the disadvantage that they account for the effect of adjacent blade rows upon the velocity distributions of molecules incident on an internal row in an approximate manner. The most accurate approach, consistent with the general assumptions of Chapter III, is a Monte Carlo solution for any particular set of blade rows, considered as a whole. In this respect the Monte Carlo method has its greatest advantage over other types of numerical calculations. Numerical integration techniques, at best inefficient when applied to a single row unless precision is required, offer little hope of direct solution to the problem of multiple rows.

The Monte Carlo solution was programmed for the M.I.T. I.B.M. 704 computer, allowing for any number of rows of alternating rotors and stators with the initial and final row either a rotor or stator. All rows are geometrically similar (the same s/b and α) with identical rotor blade speed ratios, S , and a constant flow area; provision was made for finite blade thickness. As before, the blades are flat plates and molecules incident upon the compressor from the adjacent gas are assumed to have a Maxwellian velocity distribution specified by S and $\beta = \pm \pi/2$.

The computation proceeds in the same manner as the single-row calculation, with the results expressed in terms of overall transmission probabilities. The equations used for the single row are still applicable and only the following features merit additional comment.

When a molecule is incident from one row to another, the magnitude of its velocity relative to the first row is taken from equation A.23

if it has come directly from the Maxwellian gas outside the compressor without striking the blades. In the more usual case, where the molecule comes from a collision with a blade, equations A.3 and A.4 show that its probability of having a dimensionless speed between u and $u + du$ is proportional to

$$u^2 e^{-u^2} du .\qquad\qquad 6.12$$

One of the uniformly distributed random numbers, r_4 , can then be used to select a particular speed relative to the first row, such that

$$r_4 = \frac{\int_0^u u^2 e^{-u^2} du}{\int_0^\infty u^2 e^{-u^2} du} \qquad\qquad 6.13$$

Integration gives

$$r_4 = \text{erf } u - \frac{2}{\sqrt{\pi}} u e^{-u^2} \qquad\qquad 6.14$$

The velocity of the molecule relative to the row upon which it is incident can then be calculated using its speed and direction in the coordinate system of the first row and the blade velocity.

The remaining problem results from the low probability of transmission through the multiple rows for molecules coming from the high density side. In order to perform the computations without an excessive number of samples, a method of multiplication is used.

A molecule passing from one row to another in the direction of decreasing density is replaced by M molecules, where M is called the multiplication factor; similarly only one out of every M molecules

passing between rows in the opposite direction is considered. This is done at each of the n-1 planes between rows in an n-row compressor.

With a little thought, it can be seen that this multiplies the overall transmission probability by M^{n-1}. The number of samples must be only large enough to maintain an adequate representation of the velocity distribution between rows. With a judicious choice of M, computer time is reduced to less than one minute per blade row in most instances.

<u>Comparison of Results</u>. Calculations were made for several multiple-row compressors of constant geometry, blade speed, and flow area for which the upstream and downstream gas was considered to have a zero mean mass velocity relative to a stationary observer. Negligible blade thickness was assumed and only those configurations with a rotor on the low-density side of the compressor were used. The spacing between blade rows is unimportant as long as intermolecular collisions and collisions between molecules and the compressor housing are sufficiently rare that the velocity distribution between rows is unchanged.

Figure 11 compares the three methods outlined in this chapter for a typical geometry and for one to eight blade rows. If the multiple-row Monte Carlo computation is used as a standard of comparison, the percentage differences--per blade row--in density ratios obtained by the other methods is small, confirming the suitability of calculations based upon Maxwellian velocity distributions. This is particularly emphasized by the improvement in accuracy over the direct combination of single row results brought about by the use of equivalent Maxwellian velocity distributions.

Figures 12 through 17 show density ratio at zero flow for one to eight blade rows and several geometries and blade speeds, using the multiple-row computer calculations and direct multiplication of single-row results. Except for one case, the latter calculation gives conservative results. It can be seen that the contribution of each additional blade row to the overall density ratio reaches a more or less constant value. Interpolating between the values of the independent variables given here, an estimate can be made in any particular case of the error in the slope of these lines for calculations based upon a combination of single-row results.

A comparison of density ratio vs. flow parameter calculated from multiple-row Monte Carlo results with the characteristic of a typical oil diffusion pump is given in Figure 18.

CHAPTER VII

EXPERIMENTAL PROGRAM

Experimental Apparatus. To establish the validity of the theoretical results, an experimental apparatus, which would enable the measurement of density ratio in the free-molecule range across a single compressor rotor with flat-plate blading, was designed and built. A schematic diagram of this apparatus is shown in Figure 22 and an assembly drawing of the test section is given in Figure 23. Figures 25, 26, and 27 are photographs of the overall test facility and of the rotor.

The test section consisted of a cylindrical steel housing in which the aluminum compressor rotor was driven by a high-frequency induction motor. To maintain densities sufficiently low for free-molecule flow in the test section, the housing was mounted directly on a six-inch oil diffusion pump with its axis and the axis of the compressor rotor in a vertical direction. The shaft connection between the rotor and the induction motor was made through an annular clearance seal 0.750 inches in diameter, 0.540 inches in length, and with a radial clearance of .002 inches. Using the formula for a thin slitlike tube[1], the molecular conductance of the clearance seal is found to be 1.13×10^{-3} liters per second for air at 20°C. Thus if the pressure on the motor side of the seal is maintained at a micron or less the flow from the region of the motor is of the order of 10^{-3} micron liters per second, a negligible leak at the conditions of the tests. To accomplish this, the motor housing was connected to a two-inch oil diffusion pump. As a further precaution a low vapor-pressure silicone grease was used as a lubricant for the motor ball bearings. Provision was made to admit gas to the system both

above and below the rotor. Seals between the system and the atmosphere were maintained by means of welded and soldered joints, O-rings, special gasket seals for the ionization guages, and, in the case of the thermocouple gauges and the gas inlet tubes, by red glyptal lacquer.

The densities upstream and downstream of the compressor rotor were measured by hot filament ionization guages. One thermocouple gauge was used to insure that the pressure in the motor housing was below one micron and another was connected to the test section upstream of the disk. The flow rate of gas admitted into the system was measured on the high-pressure-side of the leak valve by the displacement of a column of mercury in essentially the same manner as that described by Dushman[2]. However, it was assumed that the mass flow rate of gas through the leak valve was proportional to the square of the pressure on the high pressure side of the valve, as for flow at low Reynolds numbers, and the flow measurement was used to determine this constant of proportionality. The speed of the rotor was measured by a permanent magnet and coil tachometer and an electronic counter. The temperature of the outer race of the bearing at the rotor end of the shaft was obtained with a thermocouple and potentiometer.

Experimental Technique. The apparatus was prepared for testing by thoroughly cleaning all surfaces to be exposed to the vacuum with acetone and by heating the entire apparatus with infrared lamps to a temperature of the order of 100°C. for several hours with the vacuum pumps operating. At zero blade speed, with both leak valves closed, a pressure of about 2×10^{-6} mm. Hg was obtained at the downstream ionization guage. A comparison of this value with the reading of the upstream ionization

gave an approximate value for the flow rate from leaks and virtual leaks in the system, using the single-blade-row calculations for a stationary rotor to determine its impedance to gas flow. Since the density ratio across a rotating blade row is a function of the upstream volume flow rate, the effect of these small leaks in the system was made negligible by admitting gas through the downstream leak valve and raising the density level in the system. Tests were conducted at density levels for which no density drop was measurable across the stationary rotor.

The dimensions of the compressor rotor used are given in Figure 24. Angular velocities in the range from 20,000 to 30,000 r.p.m. gave tip speeds from 620 to 955 feet per second. Both air and, because of its high molecular weight and low value of $\sqrt{2RT}$, Freon 114 were used in the tests. The pressure downstream of the rotor was maintained at about 10^{-4} mm. Hg by means of the lower leak valve. The flow of gas through the rotor was controlled by the upper leak valve and the flow rate was measured by the displacement of a mercury column, as previously described, and by the density drop across the compressor rotor at zero blade speed.

In the tests with Freon 114, for which no ionization guage calibration was available, it was only necessary to assume the guage response to be linear with density changes[1], since density ratios and not absolute values were required.

Comparison of Experimental and Theoretical Results. Figures 19, 20, and 21 give the results of the experimental program. Comparisons of density ratio at zero flow rate vs. blade speed ratio and density ratio vs. flow parameter with single blade row calculations show good agreement and reconfirm the validity of the assumptions used in the Monte Carlo

analysis. Blade speed ratios based on the blade tip speed and $\beta = \pm \pi/2$ were used for the theoretical calculations. Figure 21 shows, as expected, that the density ratio is independent of density level in the free-molecule range and decreases markedly with increasing density for Knudsen numbers less than about five.

In spite of the uncertainties in measurement associated with vacuum technology, the experimental results show a small but definite tendency toward higher density ratios at zero flow than those obtained from the single blade row calculations. A quantitative estimate can be made of two possible causes of this effect.

In the calculations, diffuse re-emission from the surfaces of the blades was assumed and no allowance was made for a tendency toward specular (mirrorlike) re-emission at the small angles of incidence involved. If a certain fraction of the molecules is considered to consistently undergo specular re-emission, almost all these molecules will be transmitted through the blade row from the low density side and almost none from the high-density side, with the geometry and blade speeds of the tests. Calculations based upon this approximation indicate that a tendency toward specular re-emission should increase the density ratio and that roughly four to five per cent specular re-emission would be required to account for the measured differences between experiment and theory. Recent data by Hurlbut [13] indicate that, for a molecular beam of nitrogen at 20° incidence on polished aluminum, the fraction of molecules re-emitted within $\pm$ 20° of the specular direction was greater than that predicted by the cosine law by 7% of the total number re-emitted in the quadrant, 0° to 90°, in which measurements were made. This

corresponds to about 3.5% specular re-emission. In this context it should be noted that as a result of difficulties in machining the surfaces of the blades were relatively rough and not polished.

An estimate can also be made of the effect, due to finite blade height, of the end walls of the region between the blades. Molecules striking the compressor housing, which is moving relative to the blades, will tend to be reflected to the "upper" blade surface (in Figure 1) and hence will have a better chance of leaving the blades in the favorable direction. A calculation similar to the analysis for very high blade speeds, mentioned in Chapter I, gives a zero-flow density ratio at high blade speeds of 37 for the geometry of the experimental rotor when the effects of the end walls are considered and a ratio of 33 when they are neglected. The percentage difference between these ratios is about the same as that between experimental and calculated values. In the present case this effect of the end walls appears to be the most significant cause of differences between experiment and theory.

CHAPTER VIII

SUMMARY AND CONCLUSIONS

Results of this Investigation. Axial-flow compressors operating in the free-molecule range have been shown to produce high density ratios by transmitting through the blades a much larger fraction of the molecules incident from the low-density side than from the high-density side. Singel-disk calculations indicate that for most cases the density ratio increases and the slope of the density ratio vs. flow characteristic becomes less favorable with decreasing blade angle, α, and spacing to chord ratio, s/b. The most significant effect, however, is the improvement of both density ratio and flow characteristic with increasing blade speed. Experimentally, density ratio was found to decrease significantly with increasing density in the transition from the free-molecule range.

An analysis of the multiple-blade-row calculations and experimental results confirms the suitability of the idealizations and assumptions used, particularly the application of Maxwellian velocity distributions. These results show that the information obtained by this investigation may be used to predict compressor performance with reasonable accuracy.

Compressor Design and Applications. Three general performance criteria for rarefied-gas compressors are high density ratio, high flow capacity, and ability to operate at relatively high downstream densities. For a single blade row with flat-plate blades these goals are not complimentary. For a multiple row machine, however, they can be simultaneously attained. The inlet blade rows can be designed so that they capture a large fraction of the molecules incident from the low density gas, and the outlet rows made with at least one of the blade

dimensions as small as possible, to maintain free-molecule flow at higher densities. Most of the blade rows can then provide a high density ratio, since the volume flow rate for a partially compressed gas is small. These goals can also be achieved by special blade shapes, applied in the same manner.

The possible applications of this type of compressor to vacuum technology and various research activities are numerous. Detailed speculation along this line will be left to the reader. However, it is interesting to make a brief comparison with oil diffusion pumps, which operate under approximately the same conditions. To do this, it should first be noted that the value of $\sqrt{2RT}$ is about 1350 ft./sec. for air at 20°C. This means that blade speed ratios, S, of the order of one can be attained with air at room temperature and that $S = 2$ would be possible if the compressor were cooled to the temperature of liquid nitrogen. Values of S for other gases would depend upon their molecular weight, with increased performance for higher molecular weights. With this in mind, Figure 18 shows that relatively few blade rows are necessary to exceed the performance of a representative diffusion pump.

While the compressor has the disadvantage of being a fairly complicated high-speed machine and presumedly more expensive, it has several major advantages: ultimate vacuum is limited only by the materials from which it is constructed and may be considerably better than that attained with diffusion pumps, as is illustrated by the Pfeiffer data mentioned in Chapter I. In addition, several disadvantages of diffusion pumps are overcome. The problem of backstreaming of oil vapor, which makes diffusion pumps unacceptable in some applications, is eliminated. The compressor will also operate at any density level and requires no heating-up period.

Evaluation of the Monte Carlo Method. The Monte Carlo method provides a useful tool for the solution of problems involving the dynamics of rarefied gases and should make possible a better understanding of this area. As a result of the complexity of molecular motions, it may be the only convenient approach in many situations; this and its direct analogue with the physical model are its chief advantages. On the other hand, accuracy increases slowly with additional effort; the probable percentage error is inversely proportional to the square root of the number of samples. Thus, in any problem for which a choice exists between the Monte Carlo method and numerical integration techniques, there is an accuracy beyond which the Monte Carlo solution is uneconomical.

Recommendations for Further Study. Three areas provide immediate opportunity for continued study: the experimental program, limitations of the present analysis, and possibilities for improved blade shapes. Experimentally, the present results should be expanded, particularly for multiple blade rows. Two limitations of the analysis may be readily examined. The effect of finite blade thickness was discussed in the section on the combination of single blade row calculations; these results should be checked by applying the multiple-row computer program. In addition, a correction should be developed to account for the influence of the end walls of the flow passage between the blades as a function of the blade height.

The problem of blade shape can be treated both analytically and experimentally. Consideration should be given to blade shapes which would increase density ratios, capture a larger fraction of the molecules

incident from the low-density side, and function effectively at higher density levels--either by increasing the upper limit of free-molecule flow or by improving performance in the transition and slip flow ranges. These criteria need not be simultaneously achieved; as mentioned previously, an effective compressor could have several different kinds of blades, each performing a different function.

APPENDIX A

DERIVATION OF THE TWO-DIMENSIONAL COSINE LAW

Diffuse re-emission, as defined in Patterson[14], necessarily
implies the cosine law of re-emission. For the purposes of this
problem, it must be shown that the fraction of the molecules, leaving
a surface, which have velocities lying within the angle between θ and
$\theta + d\theta$, where θ is a plane angle from the normal to the surface, is
proportional to $\cos \theta \, d\theta$. The velocities under consideration have
components in three dimensions and lie in the "slice" which is the pro-
jection of $d\theta$ in the direction perpendicular to the plane of θ .
Molecules leaving the surface are assumed to have a Maxwellian velocity
distribution as if they come from behind the surface from a gas at rest
with respect to the surface. If u, v, and w are velocity components
in the x, y, z directions, where x is normal to the surface and y
is parallel to the intersection of the surface and the plane in which θ
is measured, the number of molecules per unit volume having velocity
components lying between u and $u + du$, v and $v + dv$, and w and
$w + dw$ is

$$c_1 \left(\frac{1}{2\pi RT} \right)^{3/2} e^{- \frac{1}{2RT} (u^2 + v^2 + w^2)} du\,dv\,dw. \qquad \text{A.1}$$

c_1 is a constant such that the number of molecules leaving the surface
is equal to the number impinging upon it. All molecules whose velocity
components lie between u, v, w and $u + du$, $v + dv$, $w + dw$ that leave
unit area of the surface per unit time may be considered to come from a
cylinder, in the imaginary gas behind the surface, having slant height
$\sqrt{u^2 + v^2 + w^2}$ and altitude u . Thus the number of these molecules

leaving unit area per unit time is

$$c_1 \, u \left(\frac{1}{2\pi RT}\right)^{3/2} e^{-\frac{1}{2RT}\left(u^2 + v^2 + w^2\right)} du\,dv\,dw . \qquad A.2$$

Transforming coordinates to $\mathcal{U}$, θ , w , where

$$u = \mathcal{U} \cos \theta$$

$$v = \mathcal{U} \sin \theta$$

$$w = w$$

the volume in velocity space $du\,dv\,dw$ transforms to $\mathcal{U}\,d\theta\,d\mathcal{U}\,dw$ and A.2 becomes

$$c_1 \left(\frac{1}{2\pi RT}\right)^{3/2} e^{-\frac{1}{2RT}\left(\mathcal{U}^2\cos^2\theta + \mathcal{U}^2\sin^2\theta + w^2\right)} \cos\theta \,\mathcal{U}^2 d\mathcal{U}\,d\theta\,dw. \qquad A.3$$

If this is rearranged and integrated with respect to $\mathcal{U}$ from 0 to ∞ and with respect to w from $-\infty$ to ∞ , we obtain the number of molecules leaving unit area per unit time whose velocities lie within θ and $\theta + d\theta$:

$$c_1 \left(\frac{1}{2\pi RT}\right)^{3/2} \left\{ \int_{-\infty}^{\infty} e^{-w^2/2RT}\,dw \int_{0}^{\infty} \mathcal{U}^2 e^{-\mathcal{U}^2/2RT}\,d\mathcal{U} \right\} \cos\theta\,d\theta. \qquad A.4$$

Since the integrals within the brackets are independent of θ , the expression A.4 is proportional to $\cos\theta\,d\theta$, as was to be shown.

APPENDIX B

INTEGRAL EQUATION

Formulation of the integral equation discussed in Chapter IV requires the definition of the following variables:

$X(x)$ = the total number of molecules per second striking a point x on the upper surface of the blade. $0 \leqslant x \leqslant b$.

$Y(y)$ = the total number of molecules per second per area striking a point y on the lower surface of the blade. $0 \leqslant y \leqslant b$.

$X'(x)$ = the number of molecules incident upon the blade row (from the left in Figure 1) striking directly at x per second per area.

$Y'(y)$ = the number of molecules incident upon the blade row striking directly at y per second per area.

$F_x(x)$ = the fraction of the molecules reflected from x which are directly transmitted through the blade row (to the right in Figure 1).

$F_y(y)$ = the fraction of the molecules reflected from y which are directly transmitted through the blade row.

$\dfrac{F_{x,y}(x,y)}{b}$ = the fraction of the molecules reflected from x which strike y directly, per unit of area at y.

$\dfrac{F_{y,x}(y,x)}{b}$ = the fraction of the molecules reflected from y which strike x directly, per unit area of area at x.

Σ_I can be given directly by

$$\Sigma_I = \frac{1}{s/b \ N_1} \left\{ \int_0^1 X \ F_x \ d(x/b) + \int_0^1 Y \ F_y \ d(y/b) \right\}.$$

B.1

Summing the molecules striking at x and y from the opposite blades and from the incident stream

$$X = X' + \int_0^1 F_{yx} \, Y \, d(y/b) \qquad\qquad \text{B.2}$$

and

$$Y = Y' + \int_0^1 F_{xy} \, X \, d(x/b) . \qquad\qquad \text{B.3}$$

Combining A.6 and A.7

$$X = X' + \int_0^1 F_{yx} \left[Y' + \int_0^1 F_{xy} \, X \, d(x/b) \right] \, d(y/b)$$

or

$$X = X' + \int_0^1 F_{yx} \, Y'd(y/b) + \int_0^1 K_x \, (x,\xi) \, X \, (\xi) \, d\xi \qquad\qquad \text{B.4}$$

where

$$K_x(x,\xi) = \int_0^1 F_{yx} \, (\eta, \, x) \, F_{xy} \, (\xi ,\eta) \, d\eta . \qquad\qquad \text{B.5}$$

Equation B.4 is a Fredholm integral equation of the second kind[16] and the kernel, $K_x(x,\xi)$, is an elliptic integral of the first kind[17]. A solution of B.4 could be substituted into B.3 and the results, used with B.1 for Σ_I and similar equations for the mean velocities of the leaving molecules, would produce the desired solution.

The functions involved in the preceding equations may be obtained from suitable integrations of the cosine law and the Maxwellian velocity distribution.

$$X'(x) = \frac{n\sqrt{2RT}}{\pi} e^{-S^2} \int_0^{\delta_x} \sin\theta \left[e^{a^2}\left(a^2\frac{\sqrt{\pi}}{2} - a + \frac{\sqrt{\pi}}{4}\right) \right] d\theta \qquad \text{B.6}$$

where $a = S\sin(\theta - \alpha - \beta)$

and $\delta_x = \tan^{-1}\left[s/b \sin\alpha / (s/b \cos\alpha + x/b) \right]$.

$$Y'(y) = \frac{n\sqrt{2RT}}{\pi} e^{-S^2} \int_0^{\delta_y} \sin\theta \left[e^{a'^2}\left(\frac{\sqrt{\pi}}{2} a'^2 - a' + \frac{\sqrt{\pi}}{4}\right) \right] d\theta \qquad \text{B.7}$$

where $a' = -S\sin(\theta + \alpha + \beta)$

and $\delta_y = \tan^{-1}\left(\frac{s/b \sin\alpha}{y/b - s/b \cos\alpha} \right)$.

$$F_x(x) = \frac{1}{2}\left(1 - \sin\epsilon_x \right) \qquad \text{B.8}$$

where $\epsilon_x = \tan^{-1}\left(\frac{s/b \sin\alpha}{x/b - s/b \cos\alpha} \right)$.

$$F_y(y) = \frac{1}{2}\left(1 - \sin\epsilon_y \right) \qquad \text{B.9}$$

where $\epsilon_y = \tan^{-1}\left(\frac{s/b \sin\alpha}{s/b \cos\alpha + y/b} \right)$.

$$F_{xy}(x,y) = F_{yx}(y,x) = \frac{\frac{1}{2}\left(\frac{s}{b}\sin\alpha \right)^2}{\left[\left(\frac{x}{b} - \frac{y}{b}\right)^2 + \left(\frac{s}{b}\right)^2 + 2\left(\frac{x}{b} - \frac{y}{b}\right)\frac{s}{b}\cos\alpha \right]^{3/2}} \qquad \text{B.10}$$

Numerical solutions related to the integral equation approach may be obtained by several means for both flat-plate blades and other geometries. An iteration solution leading to the Neumann series has been mentioned in Chapter IV. In addition, if integration is replaced by summation over a finite number of intervals along the blade surfaces, a system of linear

algebraic equations, which may be solved by standard methods, is obtained. If m intervals are used in the summations, equations B.4 and B.5 become

$$X_i = X'_i + \sum_{j=1}^{m} F_{ji} Y'_j + \sum_{j=1}^{m} K_{ij} X_j \qquad \text{B.11}$$

where

$$K_{ij} = \sum_{k=1}^{m} F_{ki} F_{jk} \qquad \text{B.12}$$

and $i=1, 2, ---, m$.

Equations B.11 and B.12 represent m equations in which the m X_i's are unknowns. Finally, a numerical solution may be obtained using the F_{xy}'s as influence coefficients and accounting for the fate of groups of molecules striking successive points along the blade surfaces until the fraction of molecules remaining within the blades is small. The coefficient F_{xy}, F_x, F_y, X', and Y' used in the above methods may be obtained from equations B.6 through B.10 or by graphical means.

If the blades are symmetrical, a simplification in these methods results when the ultimate transmission coefficient for molecules striking a particular point on the blades is used as the dependent variable. If this coefficient is $T_x(x)$ for the upper surface and $T_y(y)$ for the lower surface, the following equations may be written

$$T_x = F_x + \int_0^1 F_{xy} T_y \, d(y/b) . \qquad \text{B.13}$$

The symmetry condition

$$T_y = 1 - T_x(1-y/b) \qquad \text{B.14}$$

allows B.13 to be written

$$T_x = F_x + \int_0^1 F_{xy} \, d\, y/b - \int_0^1 F_{xy}(x, \xi) \, T_x \, (1-\xi) \, d\xi \, . \qquad \text{B.15}$$

Setting $\eta = 1-\xi$ and noting that

$$\int_0^1 F_{xy} \, d\, y/b = 1 - \left[F_x + F_y \, (1 - x/b) \right] \, , \quad \text{B.15}$$

becomes

$$T_x = 1 - F_y \, (1 - x/b) - \int_0^1 F_{xy} \, (x, 1-\eta) \, T_x(\eta) \, d\eta \, . \qquad \text{B.16}$$

Σ_I may be found by integrating

$$\Sigma_I = b \int_0^1 T_x \, X' \, d(x/b) + b \int_0^1 T_y \, X' \, d(y/b) \qquad \text{B.17}$$

where T_y is obtained from B.14.

Comparing B.16 with B.4, it is seen that both equations are integral equations of the same type. However, the kernel of B.16 (B.10) is expressed in closed form rather than as an elliptic integral (B.5). This simplification arises from the symmetry condition B.14 and eliminates one order of integration from the resulting numerical solutions.

In an actual numerical calculation, the dependent variable chosen and the method of computation would depend upon the blade geometry, the accuracy required, the number of calculations to be made and the computational facilities available.

APPENDIX C

MONTE CARLO CALCULATIONS FOR A SINGLE BLADE ROW

Molecules incident upon the blade row are assumed to have a Maxwellian velocity distribution around a mean mass velocity, specified by V and β in Figure 1, so that the number of molecules per unit volume having velocity components lying between u and du, v and dv, w and dw is given by[9]

$$n \left(\frac{1}{2\pi RT} \right)^{3/2} e^{-\frac{1}{2RT} \left[(u - V\cos\beta)^2 + (v - V\sin\beta)^2 + w^2 \right]} du\, dv\, dw$$

If θ is an angle measured counterclockwise from the axial direction (as is β), the number of molecules per second per area crossing the plane on the left of the blade row whose velocities lie in the angle θ to $\theta + d\theta$ can be shown by a suitable integration of A.14 to be

$$\frac{n\sqrt{2RT}}{2\pi} \left[\left(\frac{1}{2} + S'^2 \right) \sqrt{\pi}\, (1 + \text{erf } S')\, e^{-S''^2} + S'\, e^{-S^2} \right] \qquad \text{C.2}$$

where

$$S = V / \sqrt{2RT}$$
$$S' = S\cos(\theta - \beta)$$
$$S'' = S\sin(\theta - \beta).$$

Dividing by the total number of molecules per second per area crossing this plane, N, as given in equation 3.5, one obtains $dn_{\theta \to d\theta}$, the fractional number of molecules between θ and $d\theta$.

$$dn_{\theta \to d\theta} = \frac{\left[(S'/\sqrt{\pi})e^{-S^2} + (1/2 + S'^2)(1 + \text{erf } S')\, e^{-S''^2} \right] \cos\theta\, d\theta}{e^{-S^2\cos^2\beta} + \sqrt{\pi}\, S\cos\beta \left[1 + \text{erf}(S\cos\beta) \right]} \qquad \text{C.3}$$

If an individual molecule is considered to be incident upon the blades, its position in terms of dimensionless distance between the blades is obtained by selecting one of the set of random numbers, r_1 , since the random numbers are uniformly distributed between 0 and 1 and all positions along the entering plane are equally probable. The angle, θ , which the molecule makes with the axial direction is obtained by setting

$$r_2 = \int_{-\pi/2}^{\theta} d\eta_{\theta \to d\theta} \qquad \qquad C.4$$

where r_2 is another of the random numbers and $\int_{-\pi/2}^{\pi/2} d\eta = 1$. Although C.4 cannot be integrated in closed form, a numerical integration yields θ as a function of r_2 . This information and a little geometry enables the computer to determine whether the molecule strikes the upper or lower blade surface (and, if so, where) or passes directly through the blade row. Measuring dimensionless distance to the right along the upper and lower blade surfaces by x/b and y/b, respectively: if $\tan \theta > \cot \alpha$

$$\frac{x}{b} = \frac{(s/b)\ r_1}{\sin \alpha\ (\tan \theta - \cot \alpha)} \quad . \qquad \qquad C.5$$

If $\tan \theta < \cot \alpha$

$$\frac{y}{b} = \frac{(s/b)(1 - r_1)}{\sin \alpha\ (\cot \alpha - \tan \theta)} \quad . \qquad \qquad C.6$$

And if x/b or $y/b > 1$, the molecules pass immediately through the blades.

If the molecule strikes the blades, the angle of re-emission may be determined by the cosine law. Since the number of molecules leaving the surface between θ and $\theta + d\theta$, where θ is measured from the normal

to the surface, is proportional to $\cos\theta\, d\theta$, the fraction between θ and $\theta + d\theta$ is $\frac{1}{2}\cos\theta\, d\theta$, so that the integral of this quantity between $-\pi/2$ and $\pi/2$ is unity. Then to find the angle of re-emission

$$r_3 = \int_{-\pi/2}^{\theta} \frac{1}{2}\cos\theta\, d\theta \qquad \text{C.7}$$

and $\theta = \sin^{-1}(2r_3 - 1)$ \qquad C.8

where r_3 is once again one of the set of random numbers. From this, the point of the next collision can be found, and so on, until the molecule leaves the blades. From a collision with the lower surface of a blade

$$y/b = s/b\,\cos\alpha + x/b + s/b\,\sin\alpha \left[\frac{2r_3 - 1}{1-(2r_3-1)^2}\right]. \qquad \text{C.9}$$

From a collision with the upper surface of a blade

$$x/b = y/b - s/b\,\cos\alpha + s/b\,\sin\alpha \left[\frac{2r_3 - 1}{1-(2r_3-1)^2}\right]. \qquad \text{C.10}$$

It should be noted that only the directions of the molecular velocities and not the speeds are necessary to determine whether or not the molecule is transmitted through the blades.

To find the mean velocity components of the molecules upon leaving the blades, use is made of the mean velocity component, in the plane of the paper in Figure 1, of those incident molecules crossing the plane on the left of the blades at an angle θ

$$\frac{\overline{V}_i}{\sqrt{2RT}} = \frac{S' + \left(\frac{1}{\sqrt{\pi}}\right) e^{-S'^2} (1 + \text{erf } S')}{\frac{1}{\sqrt{\pi}} S' e^{-S'^2} + (1/2 + S'^2)(1 + \text{erf } S')} \qquad \text{C.11}$$

and the mean velocity component (again in the plane of the paper in Figure 1) of those molecules re-emitted from a blade

$$\frac{\overline{V}_b}{\sqrt{2RT}} = \frac{2}{\sqrt{\pi}} \quad , \qquad \text{C.12}$$

The above expressions are obtained by suitable integration of the appropriate velocity distributions.

The velocity of a leaving molecule can then be resolved into the components u_t and v_t (transmitted) or u_r and v_r (reflected) where u and v are in the axial and tangential directions, positive away from the blades and parallel to $\beta_1 = + \pi/2$ in Figure 1, respectively. For an incident molecule which passes immediately through the blades

$$u_t = \overline{V}_i \cos \theta$$
$$v_t = \overline{V}_i \sin \theta \quad . \qquad \text{C.13}$$

For a molecule leaving a collision with the lower surface of a blade

$$u_t = (\cos \theta \cos \alpha + \sin \theta \sin \alpha) \overline{V}_b$$
$$v_t = (\sin \theta \cos \alpha - \cos \theta \sin \alpha) \overline{V}_b \qquad \text{C.14}$$

if the molecule is transmitted downstream, and

$$u_r = (-\cos \theta \cos \alpha - \sin \theta \sin \alpha) \overline{V}_b$$
$$v_r = (\sin \theta \cos \alpha + \cos \theta \sin \alpha) \overline{V}_b \qquad \text{C.15}$$

if the molecule is reflected upstream. For a molecule leaving a

collision with the upper surface of a blade

$$u_t = (\sin \theta \sin \alpha - \cos \theta \cos \alpha) \, \overline{V}_b \qquad \text{C.16}$$

$$v_t = (\sin \theta \cos \alpha + \cos \theta \sin \alpha) \, \overline{V}_b$$

if the molecule is transmitted downstream, and

$$u_r = (\cos \theta \cos \alpha - \sin \theta \sin \alpha) \, \overline{V}_b \qquad \text{C.17}$$

$$v_r = (\sin \theta \cos \alpha + \cos \theta \sin \alpha) \, \overline{V}_b$$

if the molecule is reflected upstream.

The mean mass velocity components of the equivalent Maxwellian velocity distributions U_t, V_t, U_r, V_r are related to u_t, v_t, u_r, v_t by

$$u = U + \frac{1}{2} \; \frac{1 + \text{erf } U}{\frac{1}{\sqrt{\pi}} e^{-U^2} + U(1 + \text{erf } U)} \qquad \text{C.18}$$

and

$$v = V \qquad \text{C.19}$$

where either subscript applies.

APPENDIX D

TABULATED RESULTS OF COMPUTER CALCULATIONS

SINGLE - ROW CALCULATIONS

All results except those marked with an asterisk(*) have been obtained with a sufficient number of samples that the probability of occurence of an error of 10% or greater is less than 10.96%.

s/b	S	$\beta = \pm \pi/2$	Samples/1000	Σ_I	P_I/Q_I
				$\alpha = 10°$	
0.5	0	+	5	.0558	
0.5	0.5	+	3	.082	3.00
0.5	0.5	-	12	.0273	
0.5	1.0	+	2	.152	8.84
0.5	1.0	-	15	.0172	
0.5	2.0	+	1	.335	28.6
0.5	2.0	-	24	.0117	
0.5	5.0	+	1	.600	75.0
0.5	5.0	-	6	.008*	
1.0	0	+	2	.1355	
1.0	0.5	+	1	.209	2.72
1.0	0.5	-	4	.07675	
1.0	1.0	+	1	.321	6.74
1.0	1.0	-	6	.0476	
1.0	2.0	+	1	.511	20.95
1.0	2.0	-	11	.0244	
1.0	5.0	+	1	.827	53.3
1.0	5.0	-	6	.0155*	
1.5	0	+	1	.378	
1.5	0.5	+	1	.474	1.71
1.5	0.5	-	1	.277	
1.5	1.0	+	1	.507	2.4
1.5	1.0	-	1	.211	
1.5	2.0	+	1	.648	5.76
1.5	2.0	-	3	.1123	
1.5	5.0	+	1	.917	41.3
1.5	5.0	-	6	.0222*	

s/b	S	$\beta = \pm \pi/2$	Samples/1.00
			$\alpha = 20°$
0.5	0	+	2
0.5	0.5	+	1
0.5	0.5	-	4
0.5	1.0	+	1
0.5	1.0	-	5
0.5	2.0	+	2
0.5	2.0	-	7
0.5	5.0	+	1
0.5	5.0	-	6
0.75	0.5	+	1
0.75	0.5	-	3
0.75	1.0	+	1
0.75	1.0	-	4
0.75	2.0	+	1
0.75	2.0	-	6
0.75	5.0	+	1
0.75	5.0	-	6
1.0	0	+	4
1.0	0.5	+	1
1.0	0.5	-	2
1.0	1.0	+	2
1.0	1.0	-	4
1.0	2.0	+	1
1.0	2.0	-	4
1.0	5.0	+	1
1.0	5.0	-	6
1.0	9.0	+	1
1.0	9.0	-	5
1.5	0	+	1
1.5	0.5	+	2
1.5	0.5	-	1
1.5	1.0	+	1
1.5	1.0	-	1
1.5	2.0	+	1
1.5	2.0	-	3
1.5	5.0	+	1
1.5	5.0	-	6

s/b	s	$\beta = \pm \pi/2$	Samples/1000	Σ_I	P_I/Q_I

$\alpha = 30°$

s/b	s	$\beta = \pm \pi/2$	Samples/1000	Σ_I	P_I/Q_I
0.5	0	+	1	.234	
0.5	0.5	+	1	.366	2.69
0.5	0.5	−	2	.136	
0.5	1.0	+	1	.525	5.30
0.5	1.0	−	3	.099	
0.5	2.0	+	1	.630	9.44
0.5	2.0	−	5	.0668	
0.5	5.0	+	1	.421	9.21
0.5	5.0	−	6	.0457	
1.0	0	+	1	.418	
1.0	0.5	+	1	.522	1.99
1.0	0.5	−	1	.262	
1.0	1.0	+	1	.670	4.11
1.0	1.0	−	2	.163	
1.0	2.0	+	1	.805	9.08
1.0	2.0	−	3	.0887	
1.0	5.0	+	1	.693	10.1
1.0	5.0	−	4	.06875	
1.0	0	+	1	.499	
1.0	0.5	+	1	.668	1.88
1.0	0.5	−	1	.356	
1.0	1.0	+	1	.795	3.63
1.0	1.0	−	1	.219	
1.0	2.0	+	1	.903	7.08
1.0	2.0	−	2	.1275	
1.0	5.0	+	1	.841	9.86
1.0	5.0	−	3	.0853	

$\alpha = 40°$

s/b	s	$\beta = \pm \pi/2$	Samples/1000	Σ_I	P_I/Q_I
0.5	0	+	1	.366	
0.5	0.5	+	1	.463	2.14
0.5	0.5	1	2	.2165	
0.5	1.0	+	1	.551	3.68
0.5	1.0	1	2	.150	
0.5	2.0	+	1	.549	5.49
0.5	2.0	−	3	.1003	
0.5	5.0	+	1	.367	4.62
0.5	5.0	−	4	.0795	
1.0	0	+	1	.453	
1.0	0.5	+	1	.631	1.96
1.0	0.5	−	1	.322	
1.0	1.0	+	1	.753	3.42
1.0	1.0	−	1	.220	

s/b	s	$\beta = \pm \pi/2$	Samples/1000	$\bar{s}_I$	P_I/Q_I

<center>$\alpha = 40°$ Cont'd.</center>

s/b	s	$\beta = \pm \pi/2$	Samples/1000	$\bar{s}_I$	P_I/Q_I
1.0	2.0	+	1	.772	5.38
1.0	2.0	-	2	.1435	
1.0	5.0	+	2	.6105	5.40
1.0	5.0	-	2	.113	
1.5	0	+	1	.570	
1.5	0.5	+	1	.721	1.72
1.5	0.5	-	1	.420	
1.5	1.0	+	1	.837	2.68
1.5	1.0	-	1	.313	
1.5	2.0	+	1	.863	5.01
1.5	2.0	-	2	.172	
1.5	5.0	+	2	.7475	6.15
1.5	5.0	-	2	.1215	

<center>$\alpha = 45°$</center>

s/b	s	$\beta = \pm \pi/2$	Samples/1000	$\bar{s}_I$	P_I/Q_I
$1/\sqrt{2}$	1.0	+	1	.657	3.1
$1/\sqrt{2}$	1.0	-	3	.2113	

<center>$\alpha = 1°$</center>

s/b	s	$\beta = \pm \pi/2$	Samples/1000	$\bar{s}_I$	P_I/Q_I
1.0	1.0	+	5	.0478	12.6
1.0	1.0	-	5	.0038*	

<center>$\alpha = 5°$</center>

s/b	s	$\beta = \pm \pi/2$	Samples/1000	$\bar{s}_I$	P_I/Q_I
1.0	1.0	+	2	.181	7.6
1.0	1.0	-	5	.0238*	

Multiple-Row Calculations

α	s/b	S	Number of blade rows	P	Q or Q'	P/Q or P/Q'
20°	1.0	1.0	2	.457	.033	14.0
20°	1.0	1.0	3	.466	2.26×10^{-3}	204
20°	1.0	1.0	4	.476	8.20×10^{-4}	581
20°	1.0	1.0	5	.464	4.06×10^{-5}	11,400
20°	1.0	1.0	6	.469	1.342×10^{-5}	34,900
20°	1.0	1.0	8	.470	2.64×10^{-7}	1.78×10^{6}
20°	1.0	0.5	2	.292	.066	4.42
20°	1.0	0.5	4	.241	.0064	37.7
20°	1.0	0.5	6	.281	6.63×10^{-4}	424
20°	1.0	0.5	8	.268	5.76×10^{-5}	4650
20°	1.0	2.0	2	.707	$.1985/12$	42.8
20°	1.0	2.0	4	.718	$.151/12^{3}$	8220
20°	1.0	2.0	6	.715	$.089/12^{5}$	2×10^{6}
20°	1.0	2.0	8	.708	$.089/12^{7}$	2.86×10^{8}
20°	0.5	1.0	2	3.21	.0164	19.6
20°	0.5	1.0	4	.324	2.43×10^{-4}	1333
20°	0.5	1.0	6	.305	3.17×10^{-6}	9.62×10^{4}
20°	0.5	1.0	8	.319	2.48×10^{-8}	1.29×10^{7}
20°	1.5	1.0	2	.544	.096	5.67
20°	1.5	1.0	4	.522	.012	43.5
20°	1.5	1.0	6	.560	$.416/3^{5}$	327
20°	1.5	1.0	8	.546	$.447/3^{7}$	2670
10°	1.0	1.0	2	.299	$.104/6$	17.3
10°	1.0	1.0	4	.312	$.0495/6^{3}$	1360
10°	1.0	1.0	6	.254	$.1355/8^{5}$	6.14×10^{4}
10°	1.0	1.0	8	.266	$.1190/8^{7}$	4.68×10^{6}
30°	1.0	1.0	2	.583	.05867	9.94
30°	1.0	1.0	4	.554	.00233	238
30°	1.0	1.0	6	.566	$.054/4^{5}$	1.072×10^{4}
30°	1.0	1.0	8	.561	$.047/4^{7}$	1.96×10^{5}

LIST OF FIGURES
Single-Blade-Row Calculations

DEFINITION OF VARIABLES

Figure 1.

Figure 2.

SINGLE ROW
α = 20°

s/b = 1.5
1.0
0.5

TRANSMISSION PROBABILITY, Σ

1.0 0.9 0.8 0.7 0.6 0.5 0.4 0.3 0.2 0.1 0

BLADE SPEED RATIO, $S = V_B/\sqrt{2}\,\overline{RT}$

-5.0 -3.0 -1.0 1.0 3.0 5.0

SINGLE ROW
α = 10°

s/b = 1.5
1.0
0.5

TRANSMISSION PROBABILITY, Σ

1.0 0.9 0.8 0.7 0.6 0.5 0.4 0.3 0.2 0.1 0

BLADE SPEED RATIO, $S = V_B/\sqrt{2}\,\overline{RT}$

-5.0 -3.0 -1.0 1.0 3.0 5.0

s/b = 1.5
1.0
0.5

PROBABILITY, Σ

1.0 0.9 0.8 0.7 0.6 0.5

s/b = 1.5
1.0
0.5

SION PROBABILITY, Σ

1.0 0.9 0.8 0.7 0.6 0.5
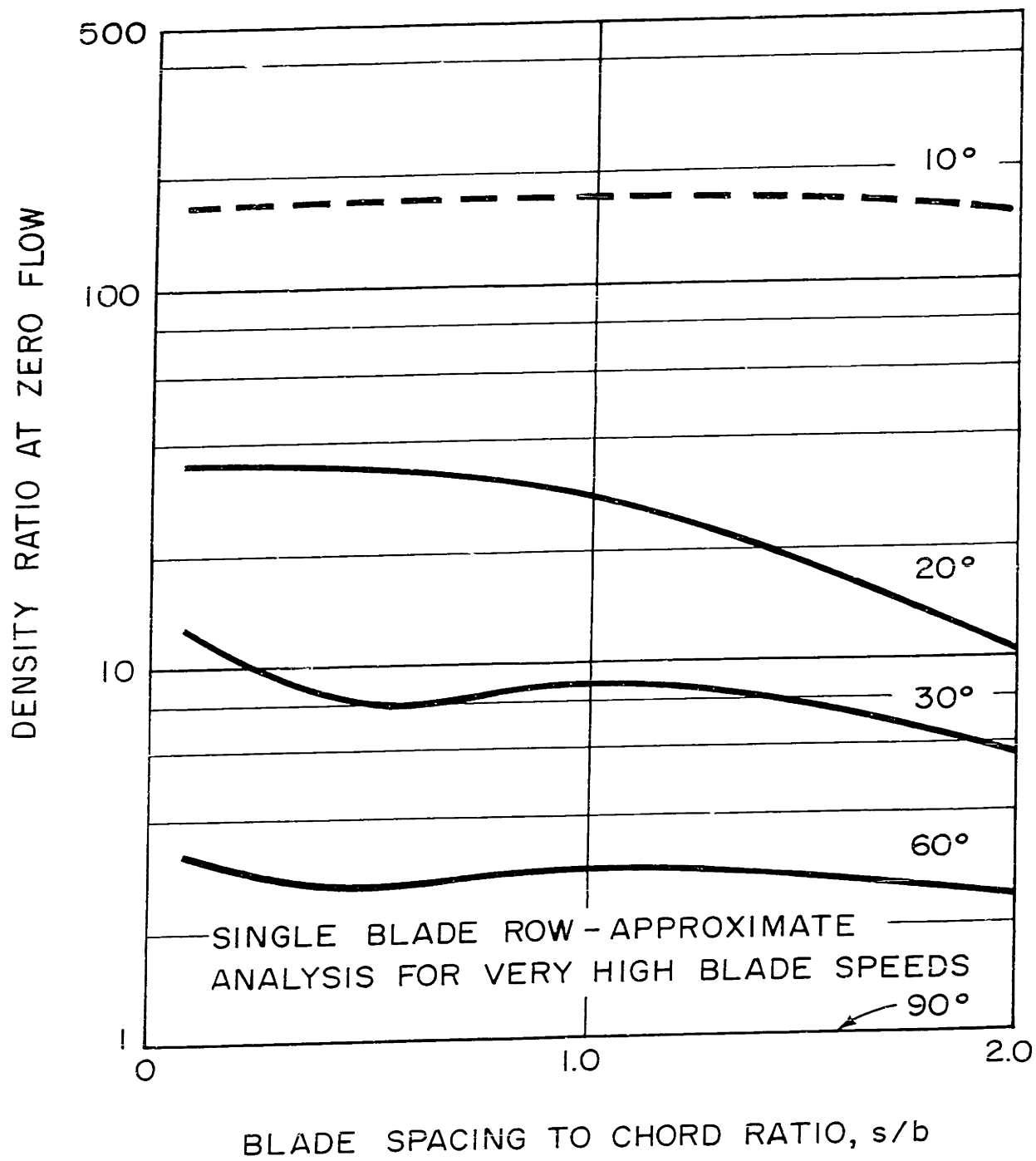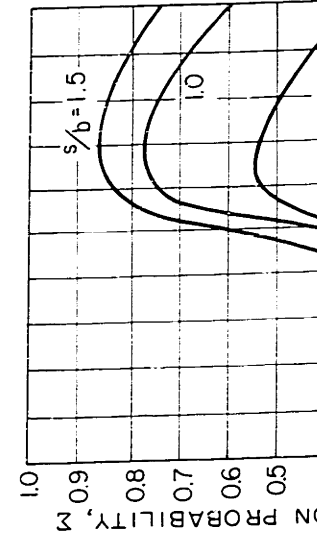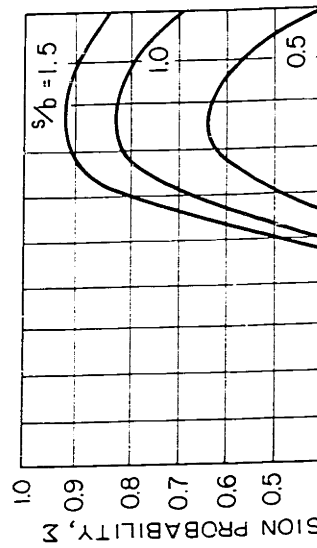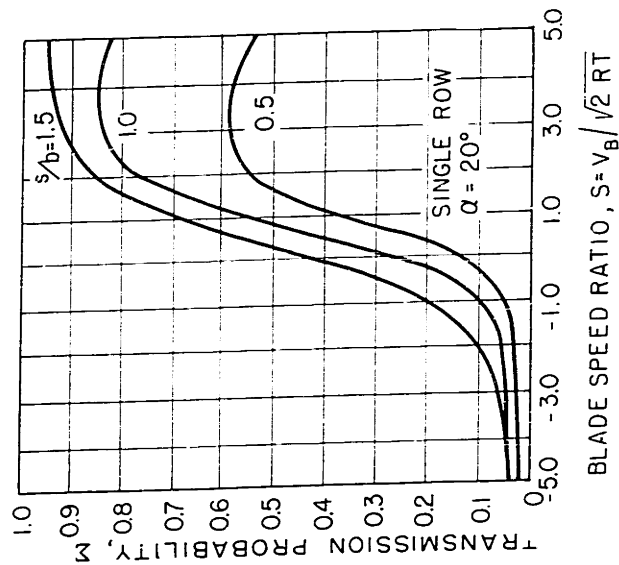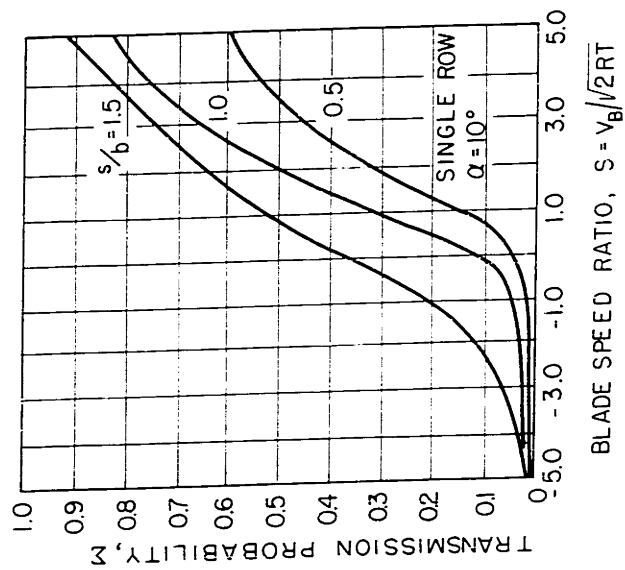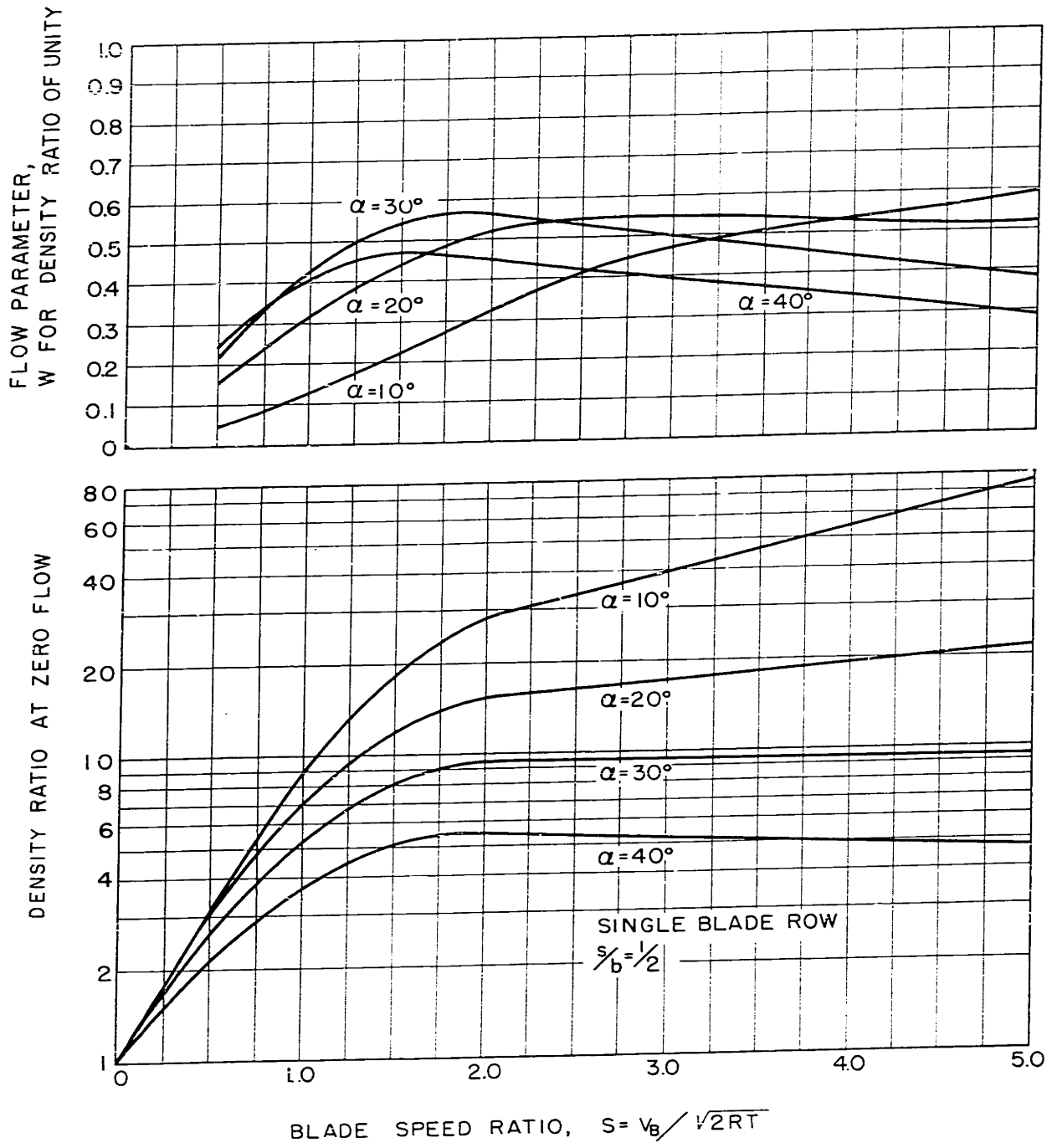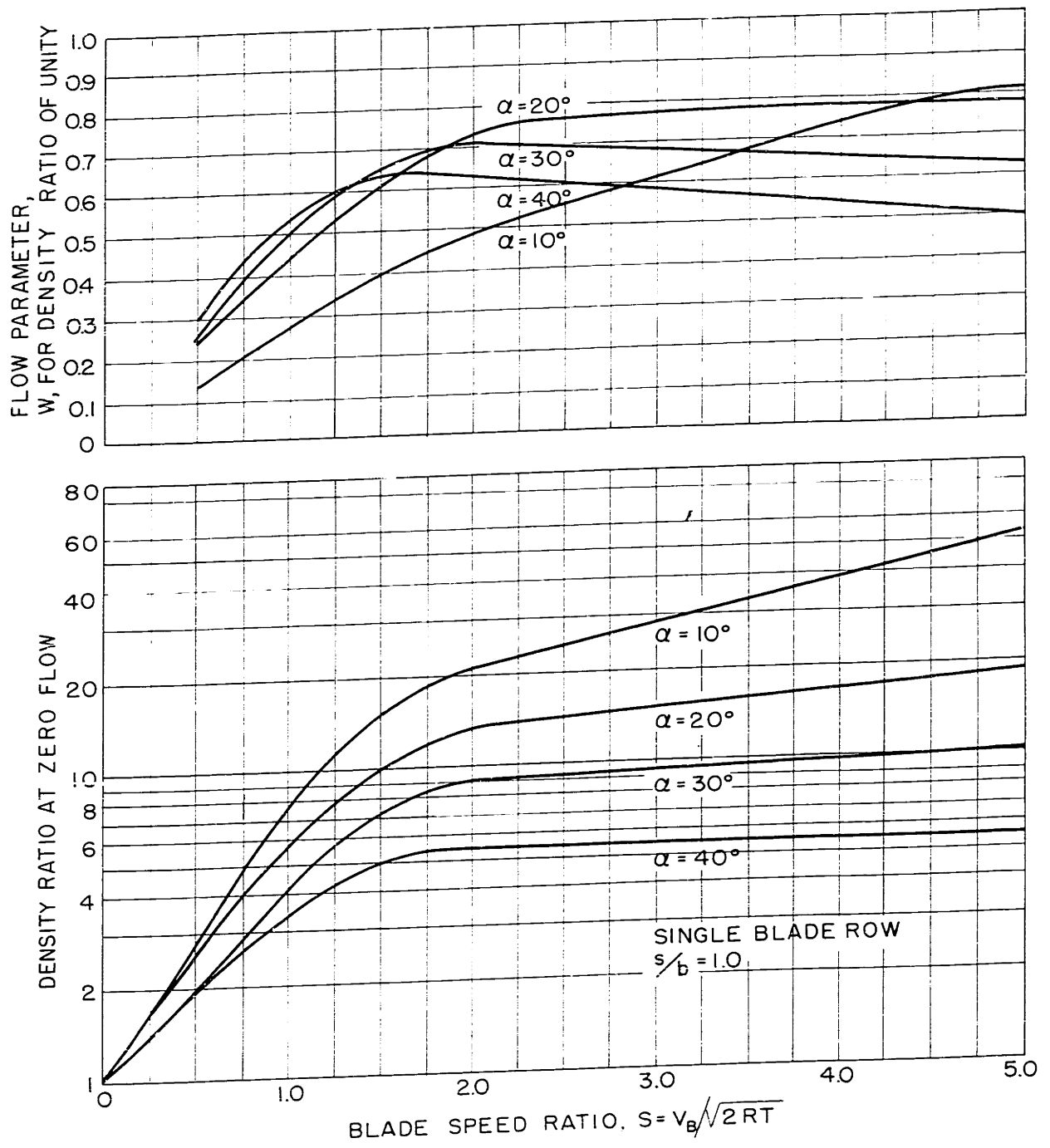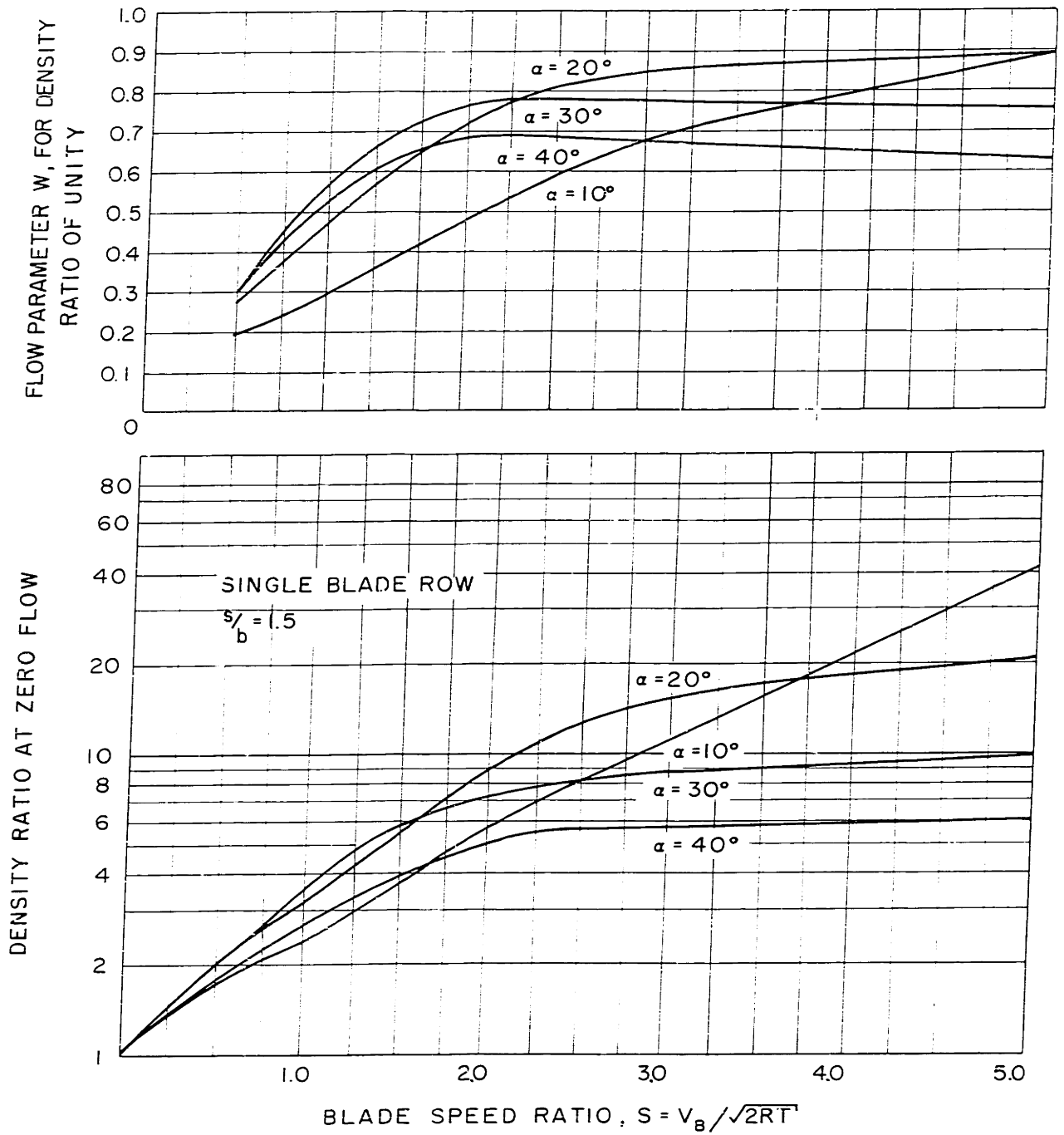
Figure 4.

Figure 5.

Figure 6.

66.
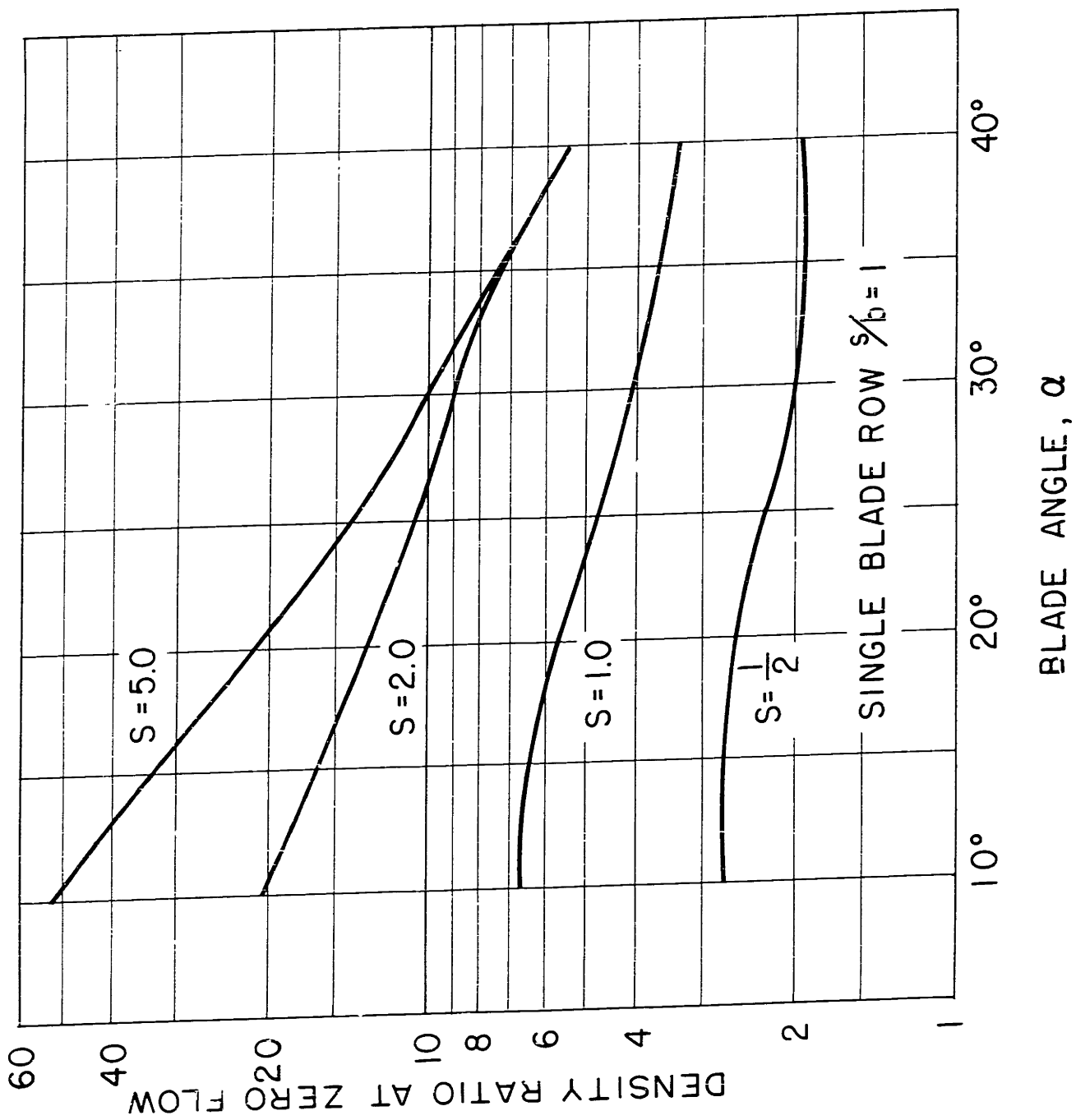
Figure 7.

BLADE SPACING TO CHORD RATIO, s/b

DENSITY RATIO AT ZERO FLOW

S=5.0

S=2.0

S=1.0

S=0.5

SINGLE BLADE ROW
α = 20°

Figure 8

SINGLE BLADE ROW

$s/b = 1.0$

$S = 1.0$

$\alpha = 10°$

$\alpha = 20°$

$\alpha = 30°$

$\alpha = 40°$

DENSITY RATIO

W, VOLUME FLOW RATE PARAMETER

Figure 9.

68.

SINGLE BLADE ROW

$\alpha = 20°$
$S = 1.0$

$s/b = 0.5$

$s/b = 1.0$

$s/b = 1.5$

DENSITY RATIO

W, VOLUME FLOW RATE PARAMETER
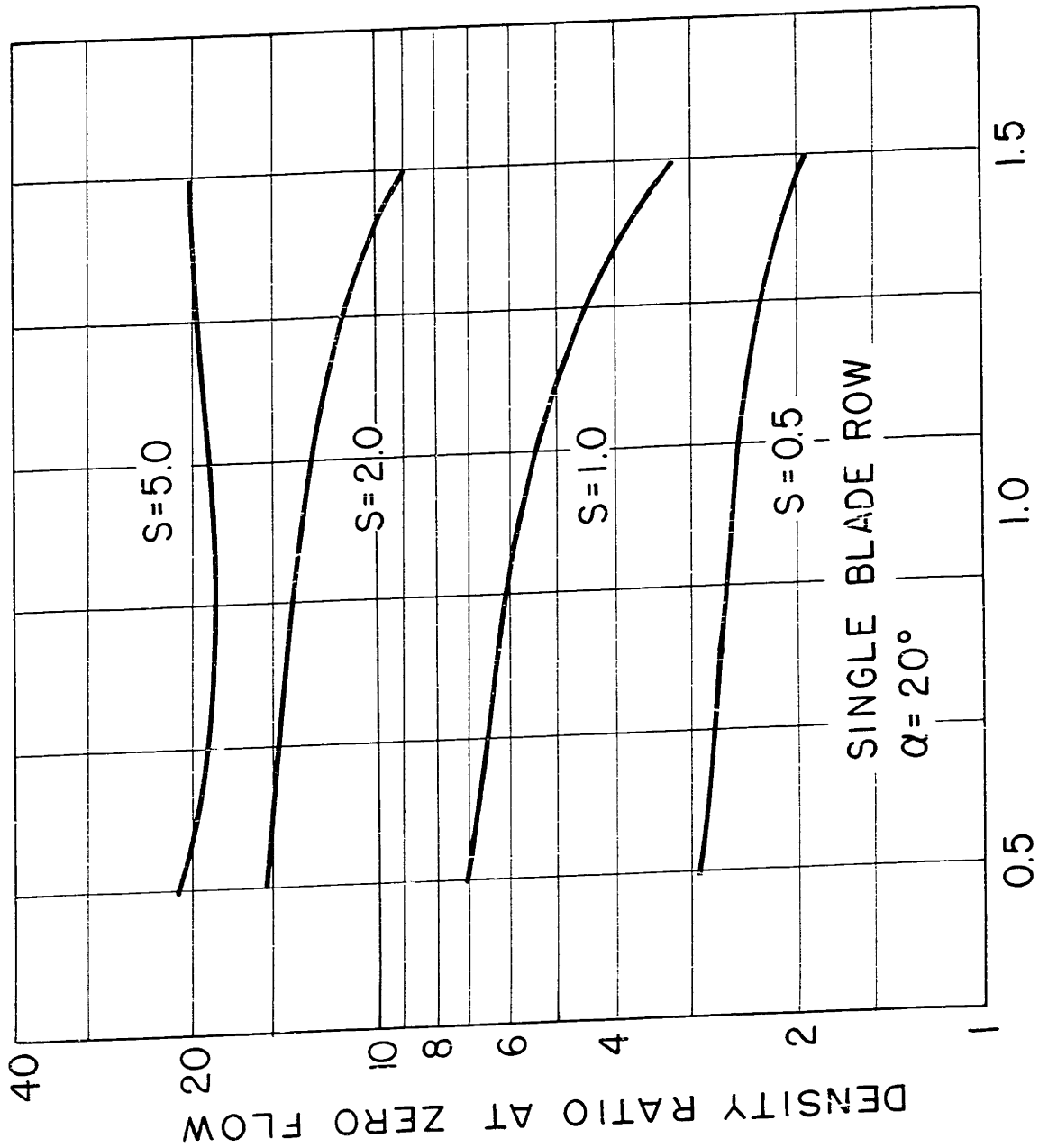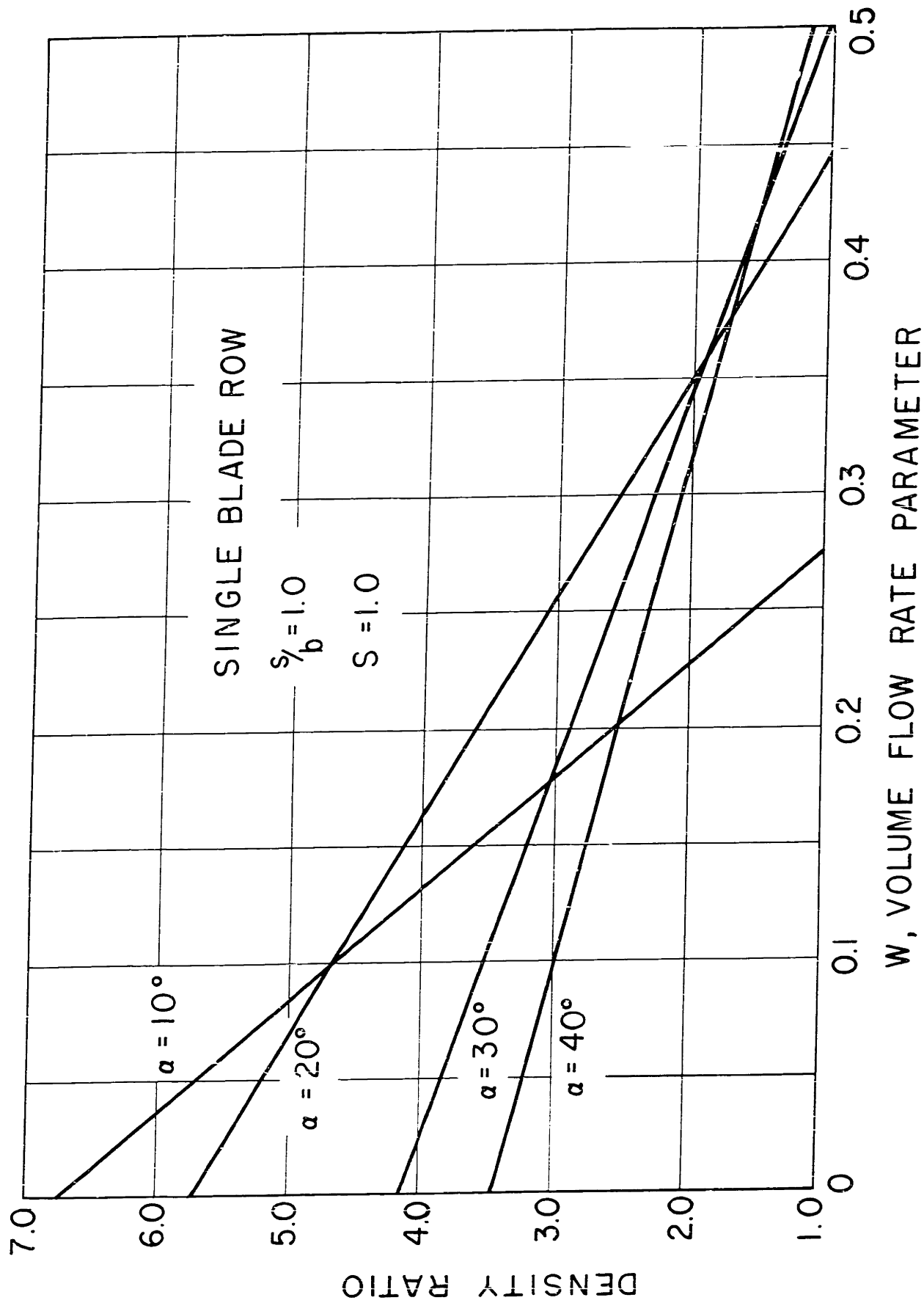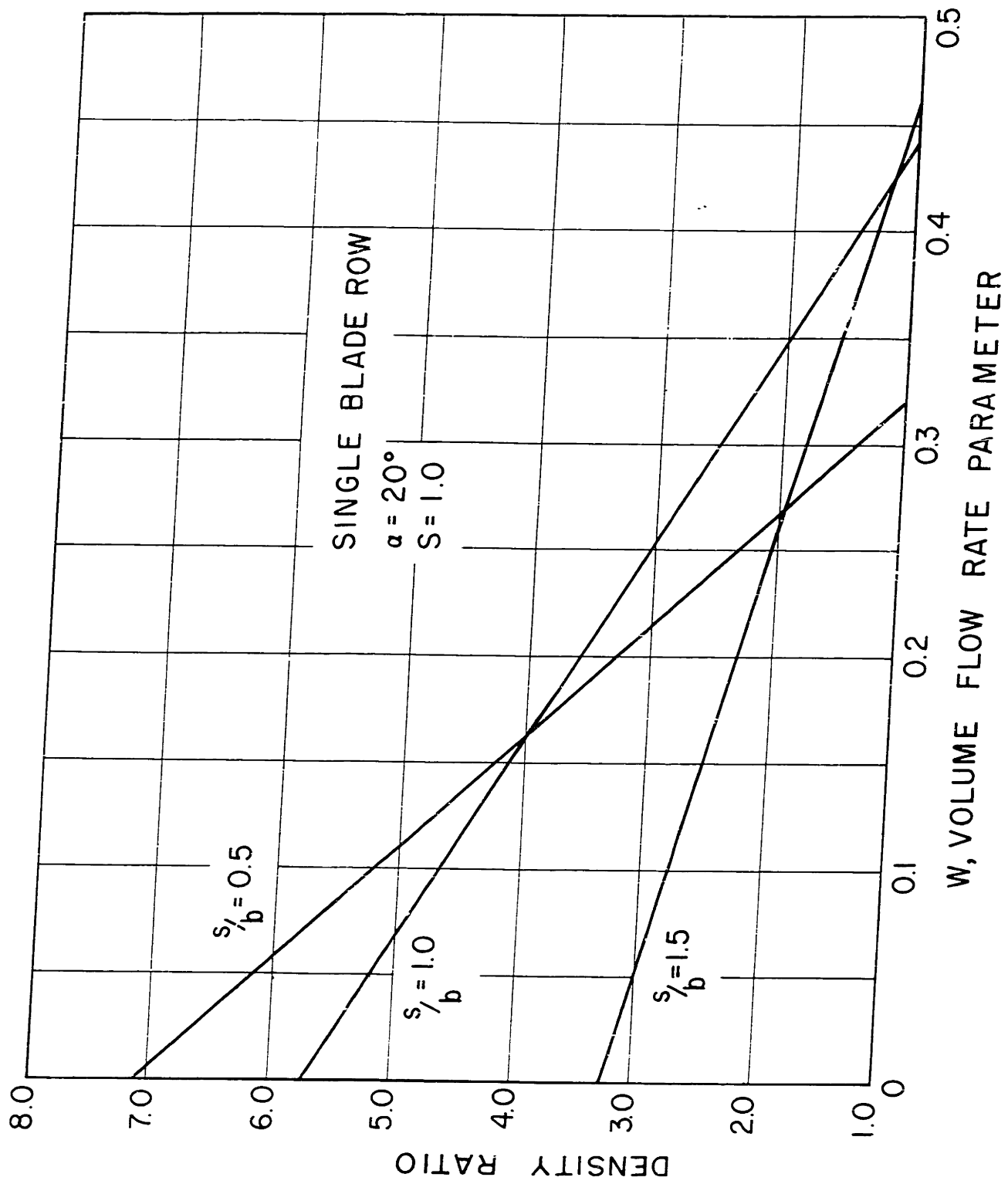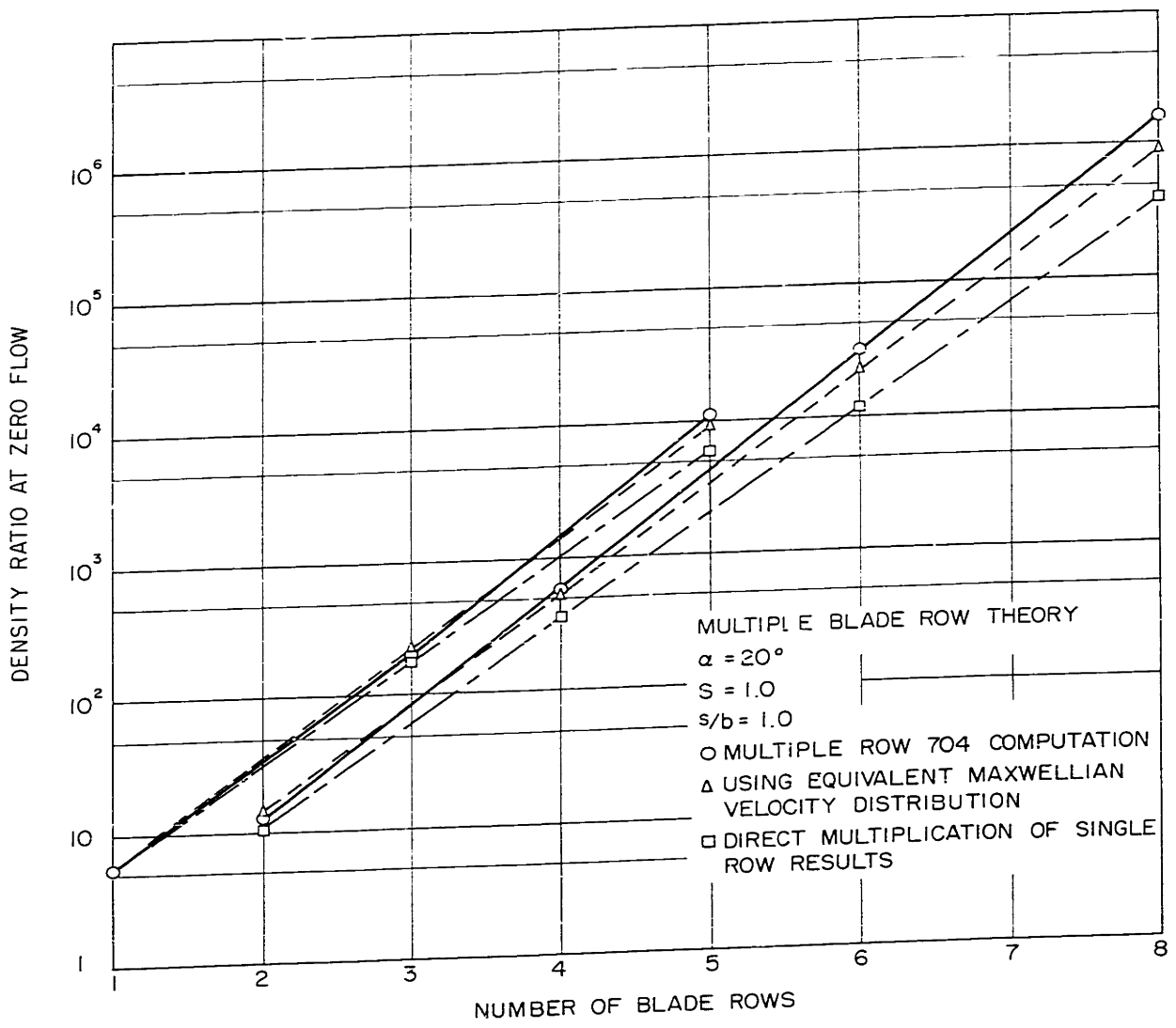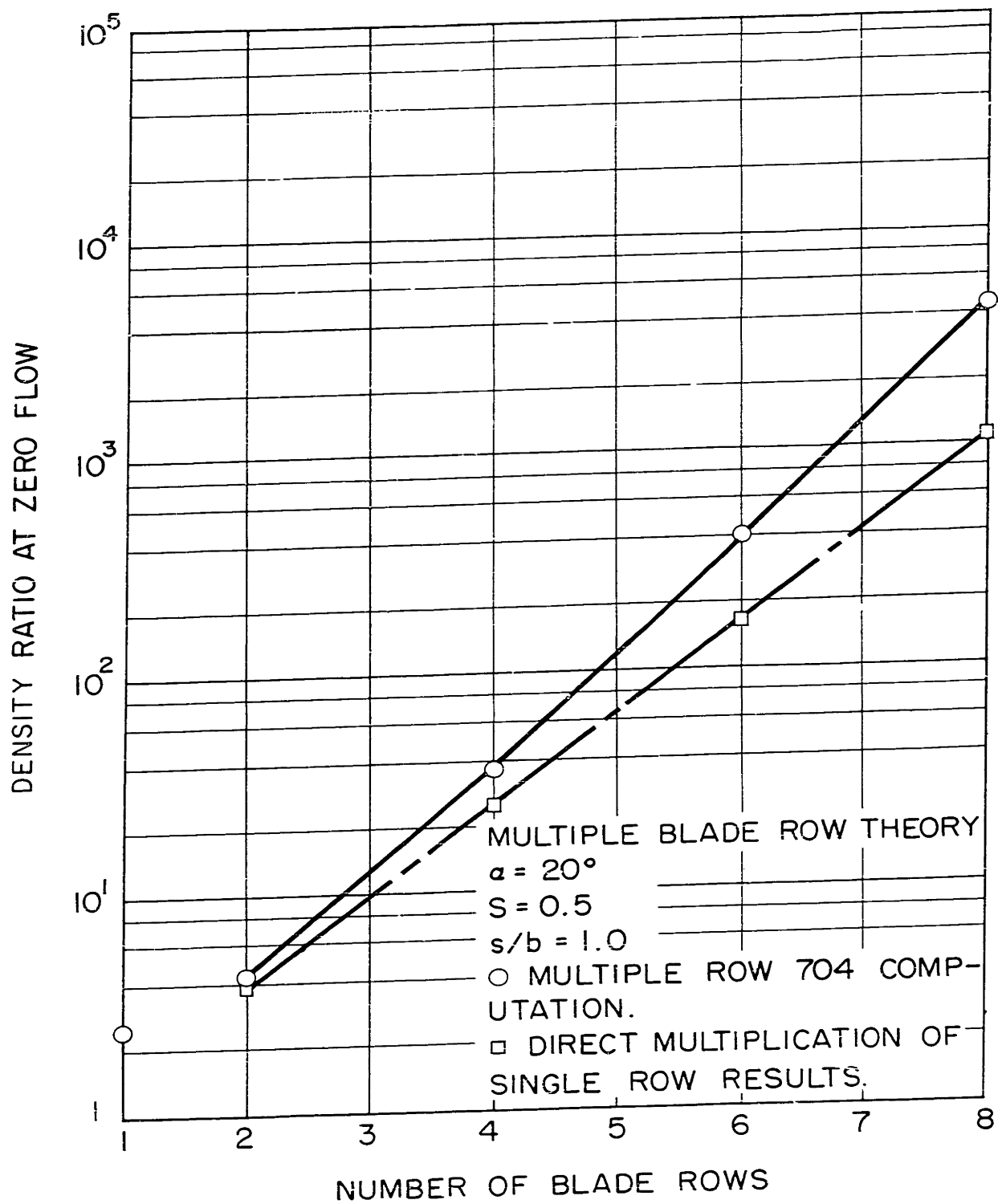
Figure 10.

Figure 11.

Figure 12.
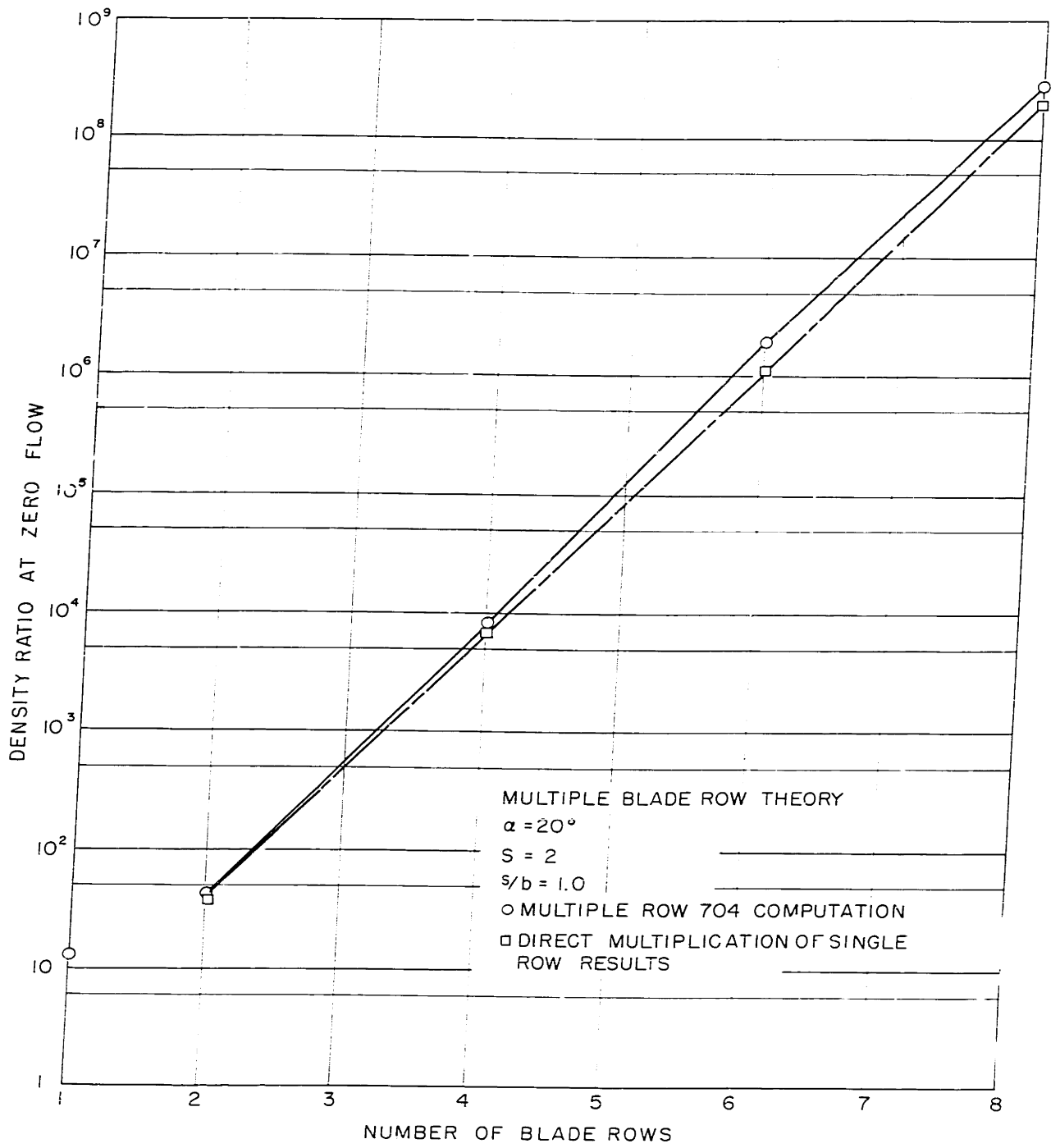
Figure 13.
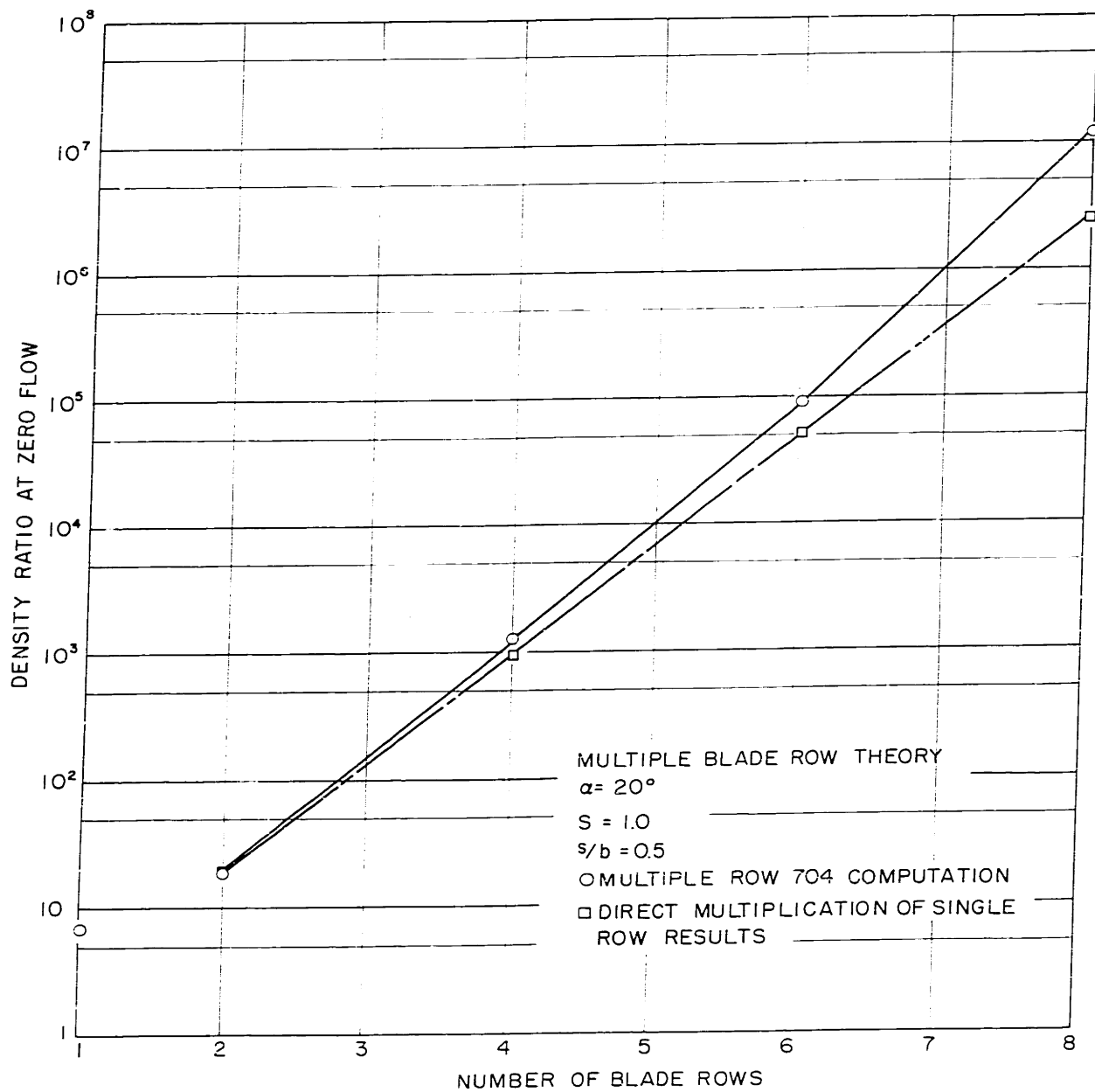
Figure 14.
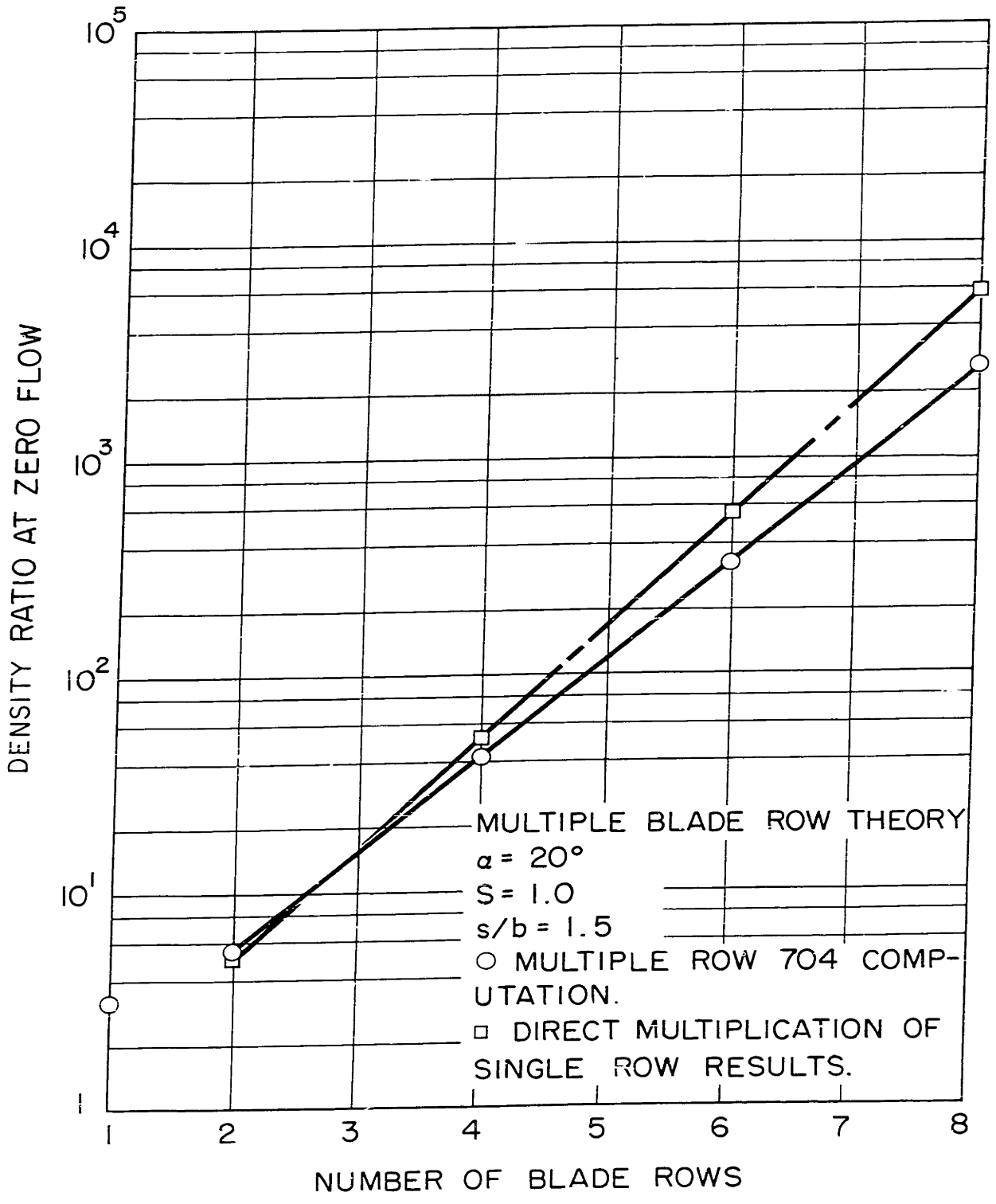
Figure 15.
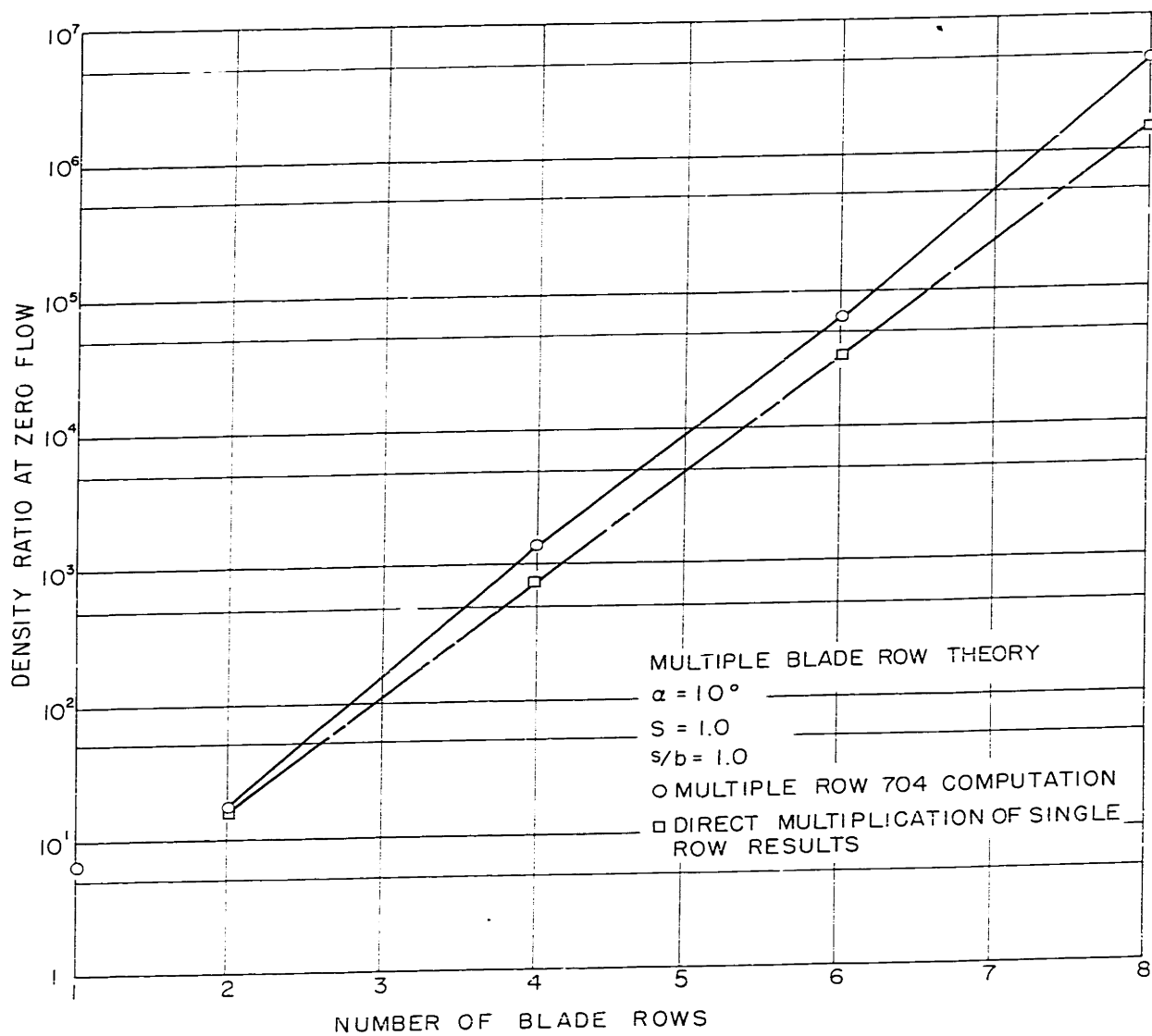
Figure 16.
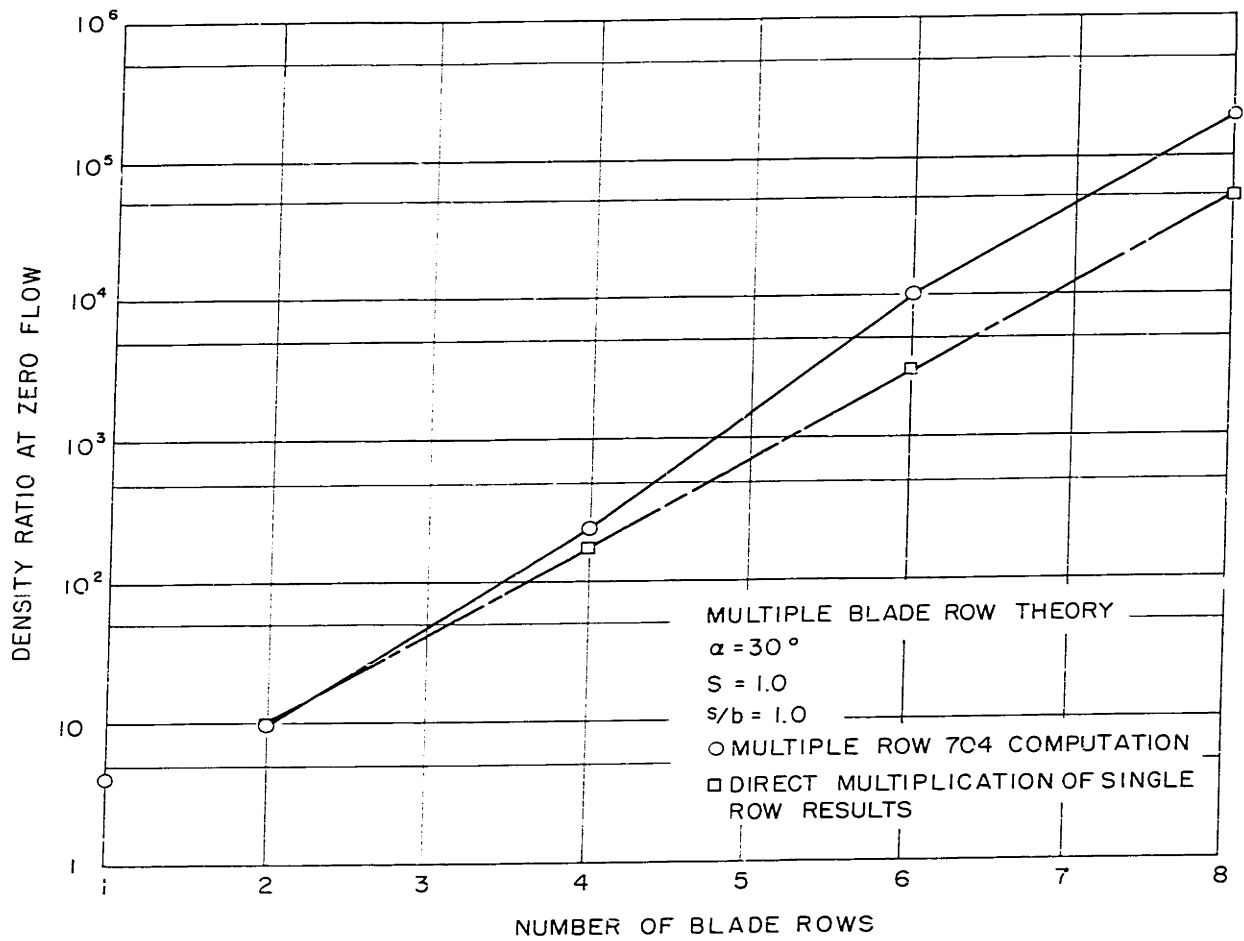
Figure 17.
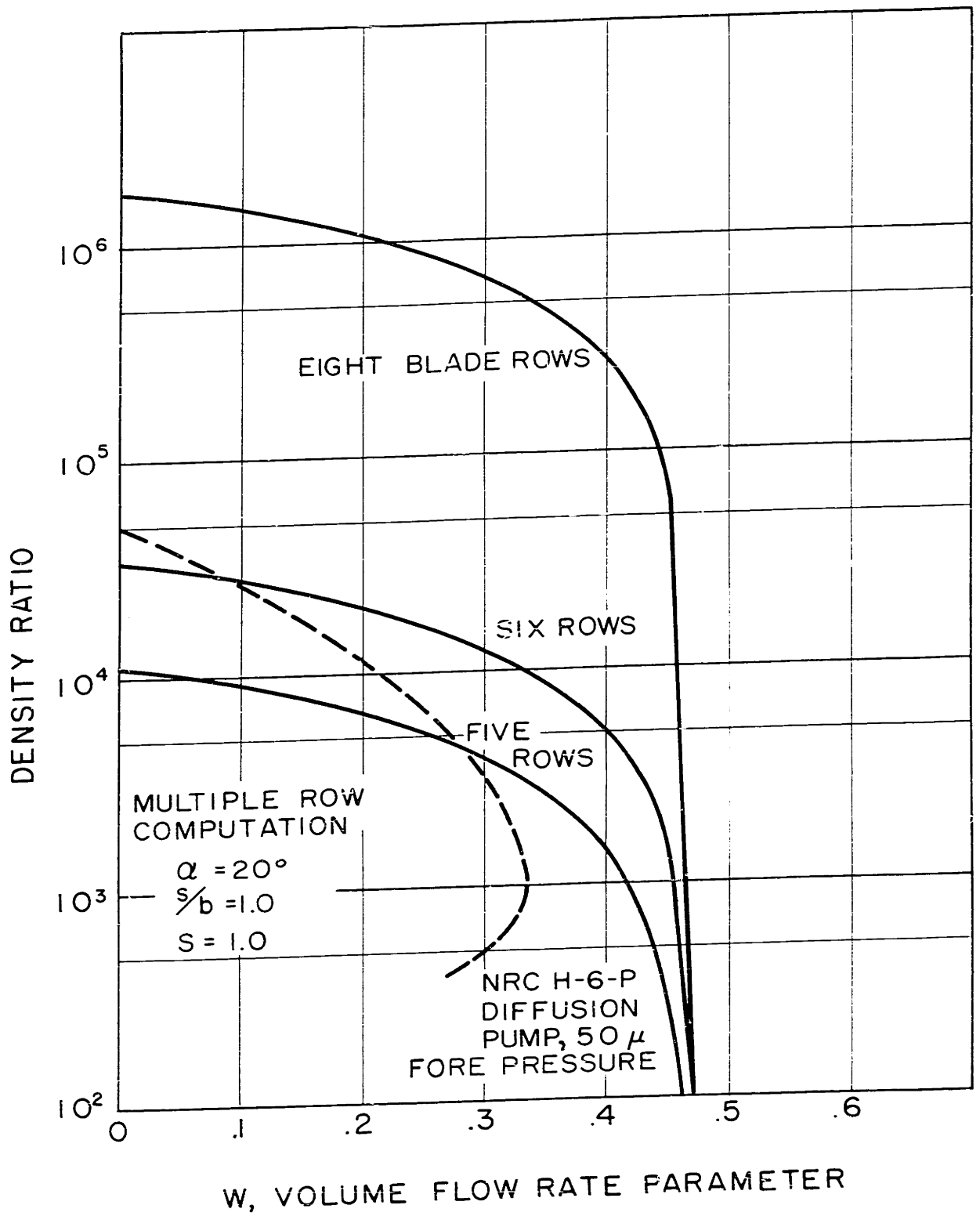
Figure 18.

Figure 19.

7
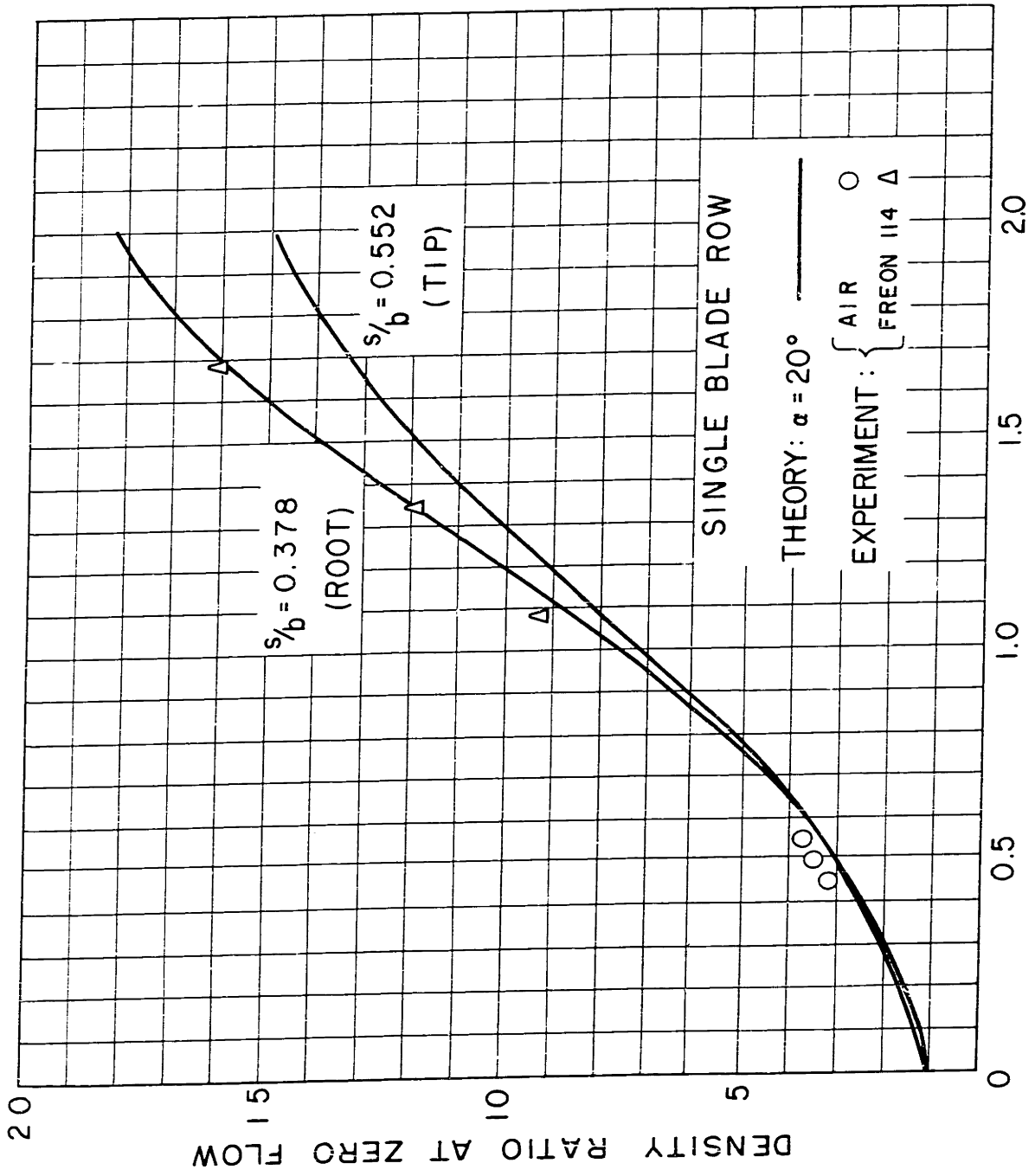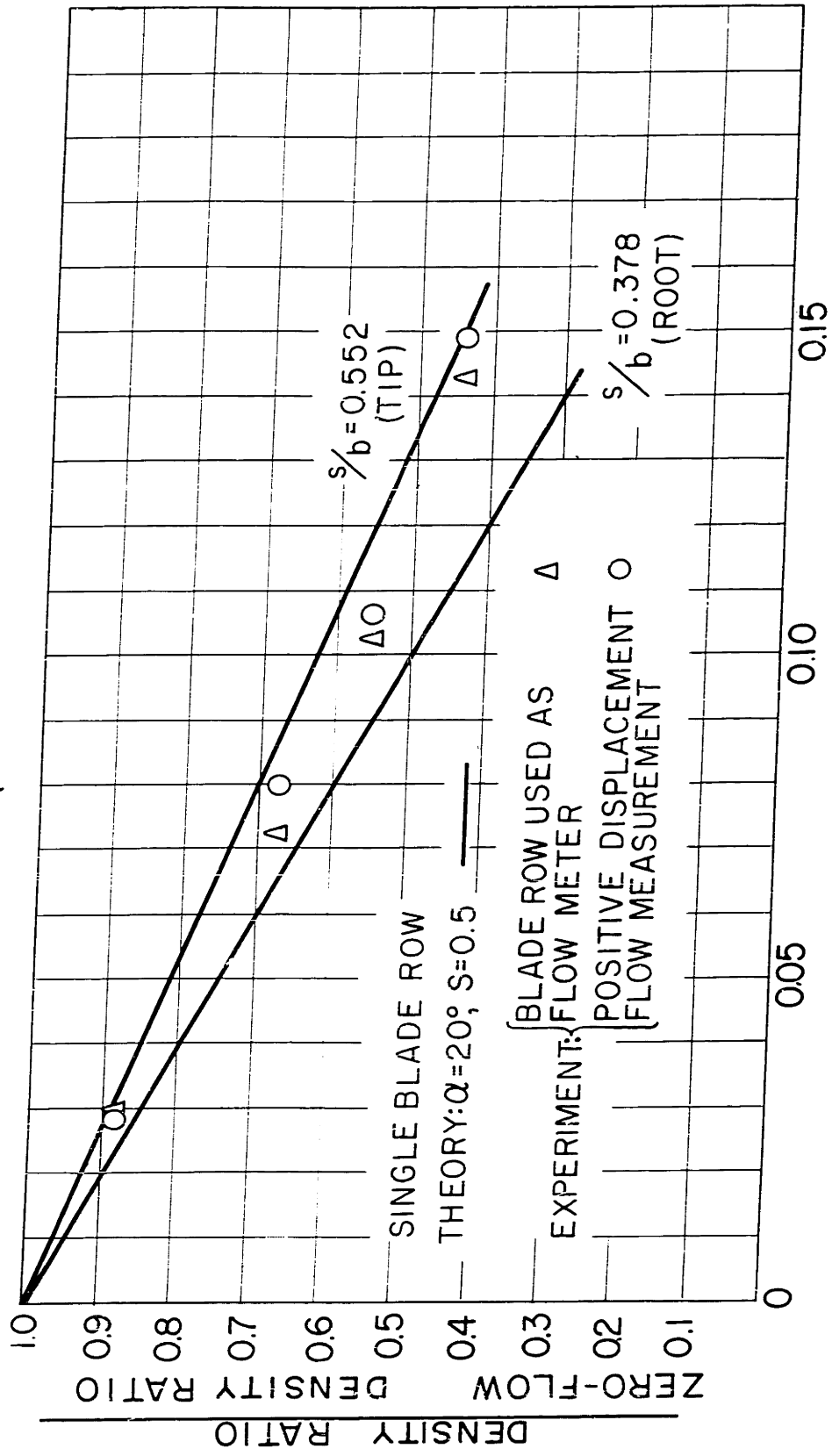
Figure 20.

KNUDSEN NUMBER, DOWNSTREAM MEAN FREE PATH/BLADE SPACING AT ROOT

MEAN EXPERIMENTAL CURVE

SINGLE ROW EXPERIMENT

$\alpha = 20°$

$S = 0.448$

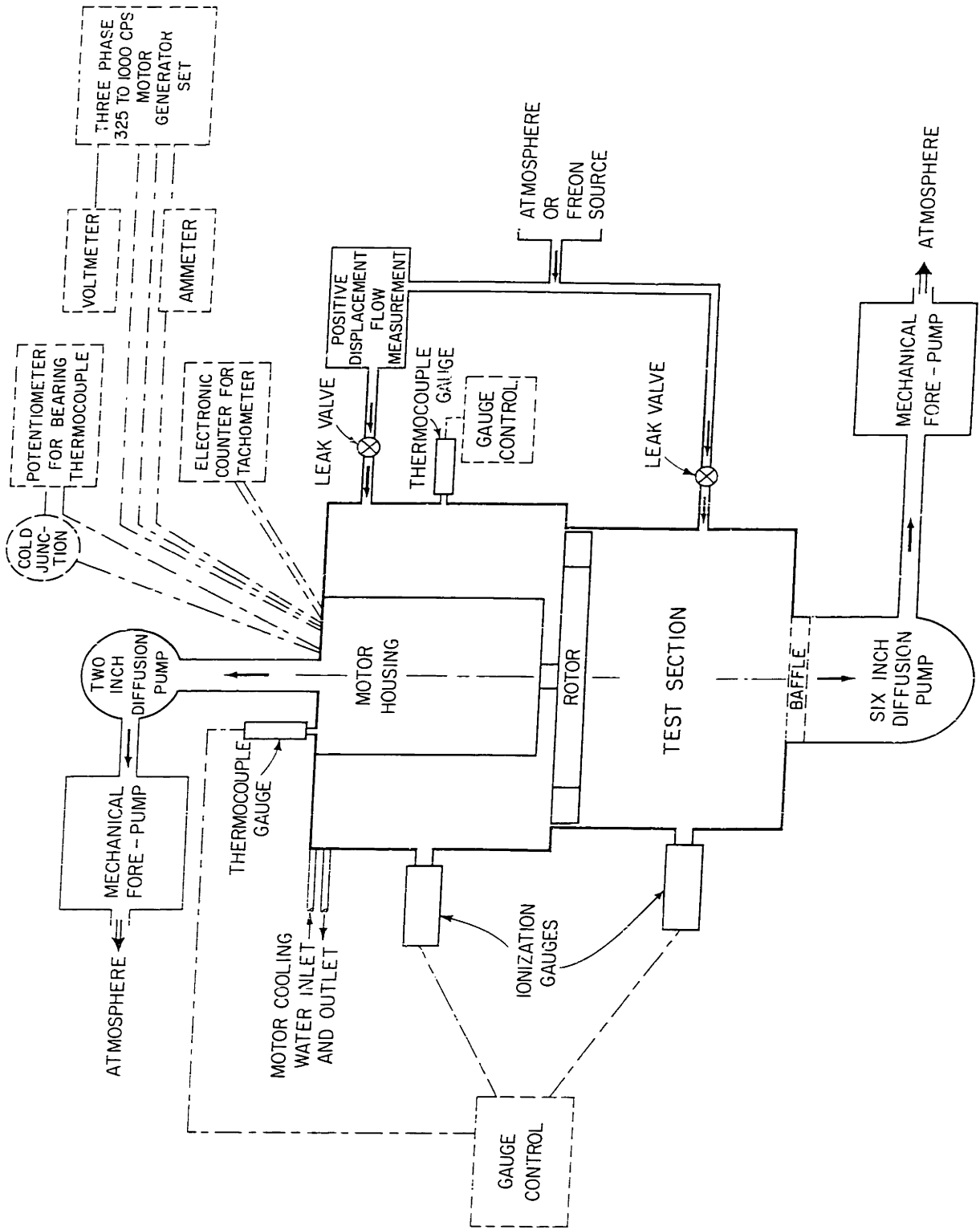$0.378 \leqslant s/b \leqslant 0.552$

DENSITY RATIO AT ZERO FLOW
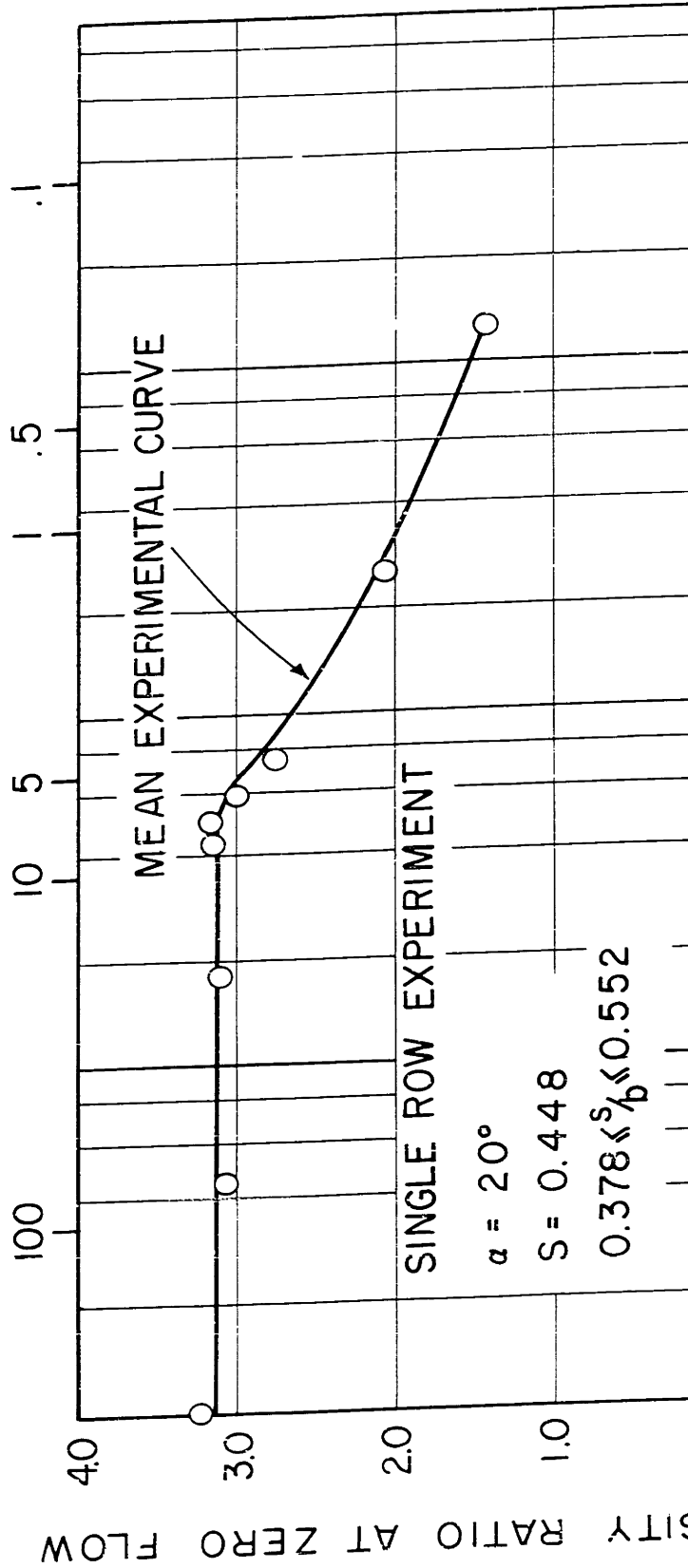
Figure 22. Schematic of Experimental Apparatus.

Figure 23. Test Section.

0.500

b = 1.462

s

$s = \begin{cases} 0.552 \text{ AT ROOT} \\ 0.808 \text{ AT TIP} \end{cases}$

0.037

α = 20°

25 BLADES

ROTOR DETAIL

9

3.650

2.545

.012

Figure 24.

84.

85.
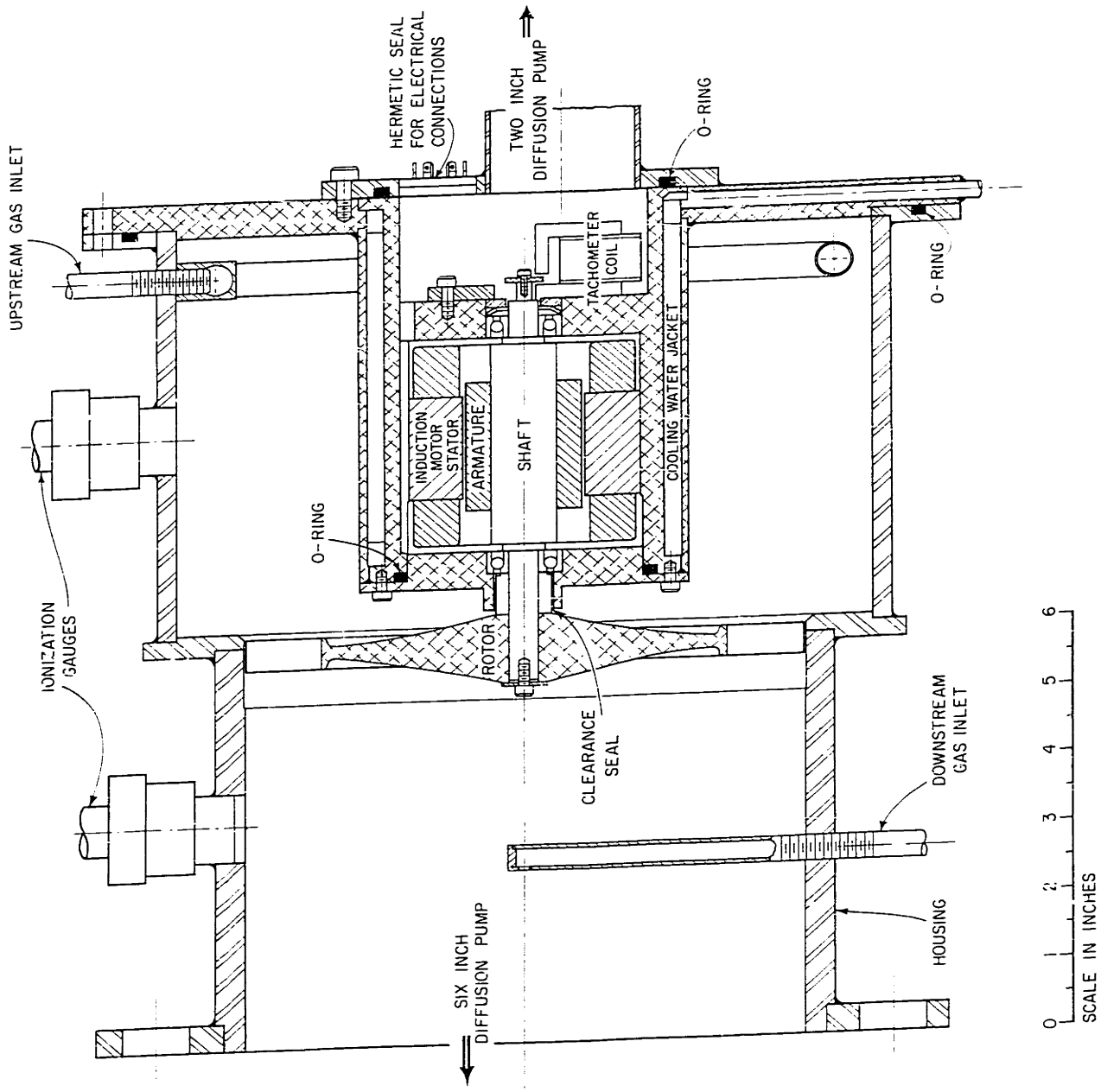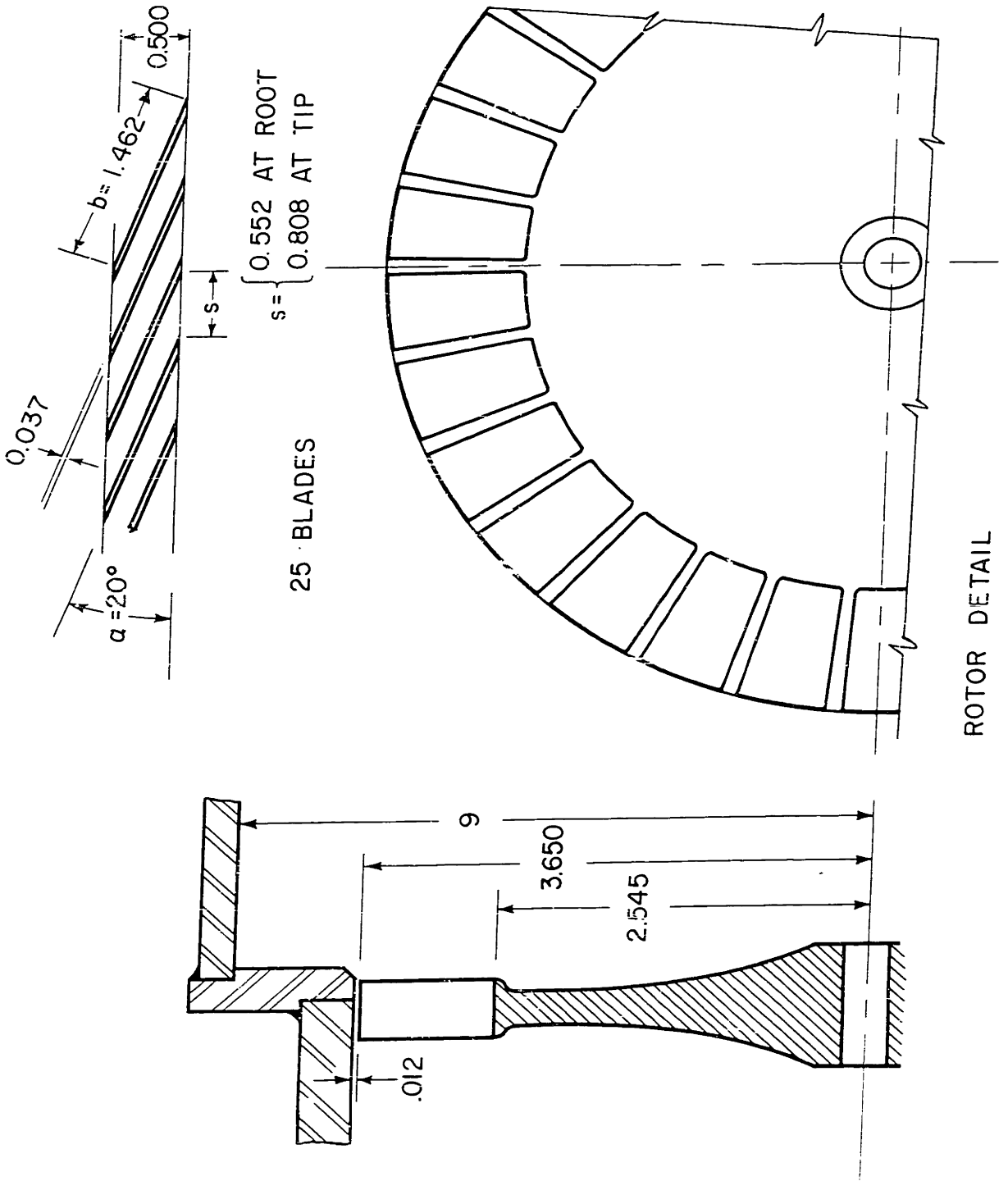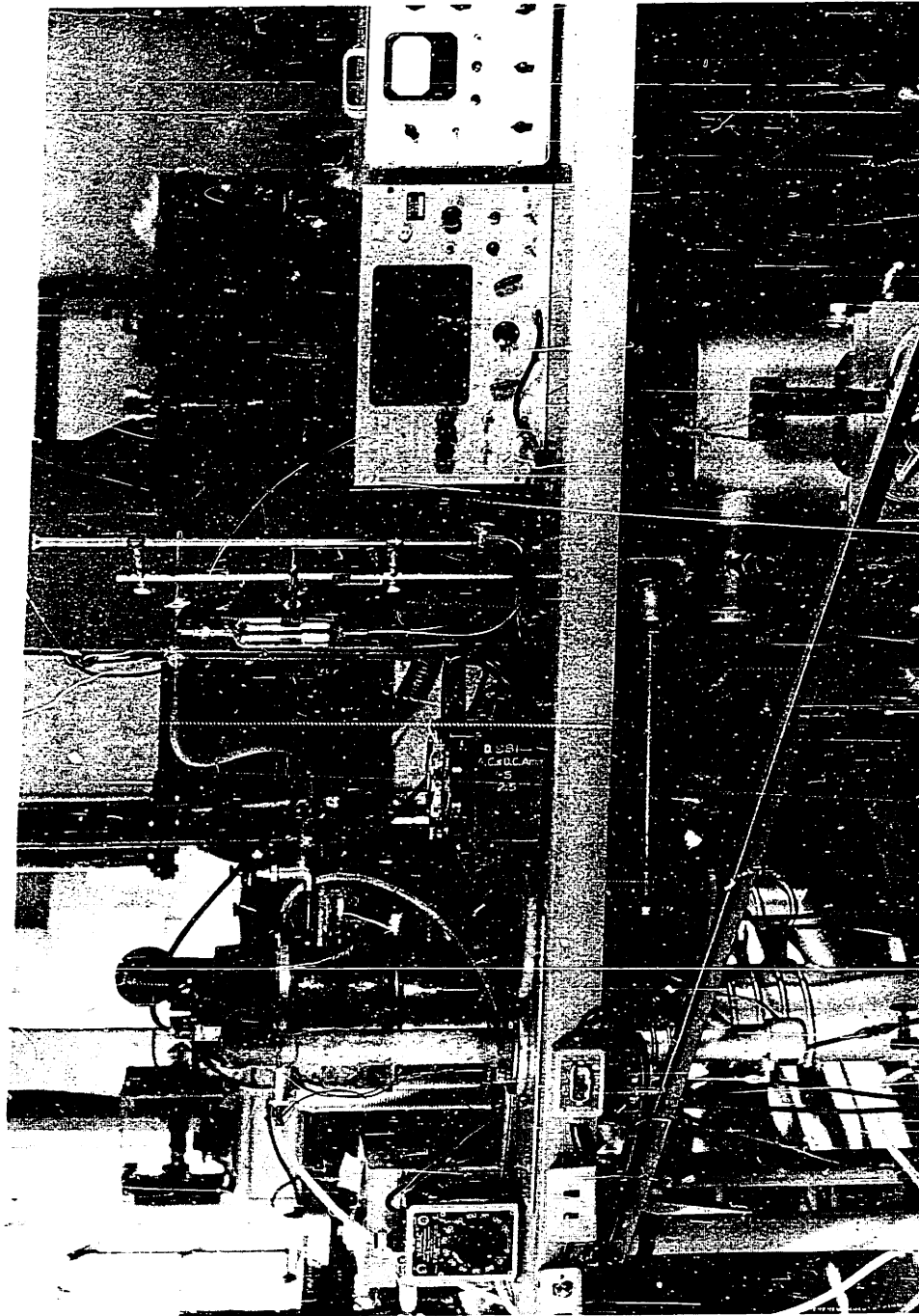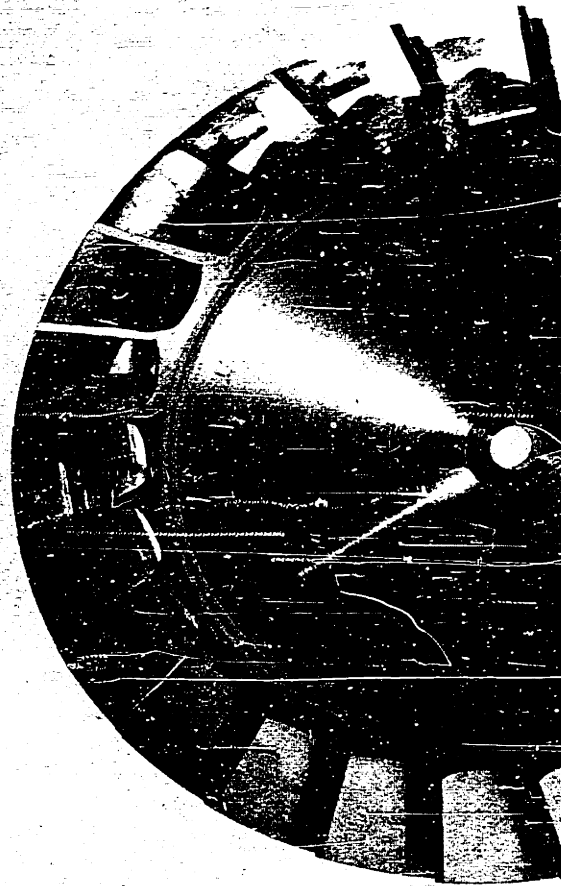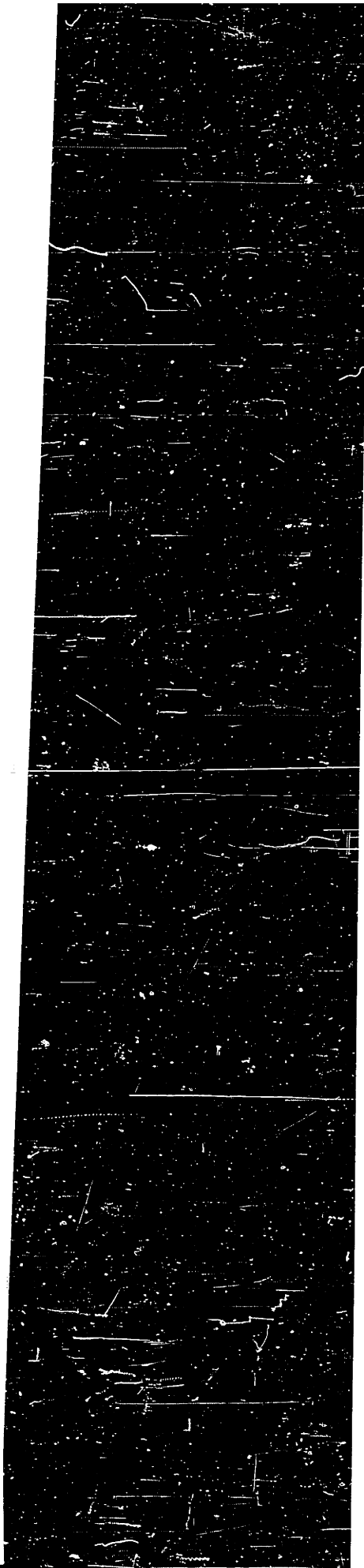

Figure 26. Compressor Rotor.

BIBLIOGRAPHY

1. Gutherie, A. and Wakerling, R. K., "Vacuum Equipment and Techniques". New York: McGraw-Hill Book Co., Inc., 1949.

2. Dushman, S., "Scientific Foundations of Vacuum Technique". New York: John Wiley & Sons, Inc., 1949.

3. Hablanian, M., "The Axial Flow Compressor as a High Vacuum Pump", First International Congress on Vacuum Technology, 1958.

4. Deutsches Patentamt Auslegeschrift 1015573, (Sept., 1957).

5. Becker, W., "Eine Neue Molekularpumpe", Vakuum-Technik, 7 Jahrgang, Heft 7 (Oktober, 1958), p. 149.

6. Finol, H. J., "Study of Free Molecule Flow Through a Cascade", S.M. thesis, Dept. of Mech. Engr., Mass. Inst. of Tech. (1958).

7. Sanger, E., "The Gas Kinetics of Very High Flight Speeds", NACA Tech. Memo., No. 1270 (1950).

8. Tsien, H. S., "Superaerodynamics, Mechanics of Rarefied Gases", Jour. Aero. Sci., Vo. 13, No. 12 (Dec., 1946), p. 653.

9. Ashley, H., "Applications of the Theory of Free Molecule Flow to Aeronautics", Jour. Aero Sci., Vol. 16, No. 2 (Feb. 1949), p. 95.

10. Kennard, E. H., "Kinetic Theory of Gases". New York: McGraw-Hill Book Co., Inc., 1938.

11. Mott-Smith, H. M., "The Solution of the Boltzmann Equation for a Shock Wave", Phys, Rev., Vol. 82, No. 6 (June 1951), p. 885.

12. Stalder, J. R., Goodwin, G., and Creager, M. O., "A Comparison of Theory and Experiment for High-Speed Free-Molecule Flow", NACA Report 1032 (1951).

13. Hurlbut, F. C., "Molecular Scattering at the Solid Surface"; Recent Research in Molecular Beams (edited by I. Estermann). New York: Academic Press, 1957.

14. Patterson, G. N., "Molecular Flow of Gases". New York: John Wiley & Sons, Inc., 1956.

15. Jahnke, E. and Emde, F., "Tables of Functions with Formulae and Curves". New York: Dover Publications, 1945.

16. Hildebrand, F. B., "Methods of Applied Mathematics". Englewood Cliffs, N. J.: Prentice-Hall, Inc., 1952.

17. Byred, P. F. and Friedman, M. D., "Handbook of Elliptic Integrals for Engineers and Physicists", Berlin: Springer-Verlag, 1954.

18. Ulam, S., "On the Monte Carlo Method; Proceedings of the Second Symposium of Large Scale Digital Computing Machinery". Cambridge: Harvard Univ. Press, 1951.

19. Meyer, H. A., ed., "Symposium on Monte Carlo Methods". New York: John Wiley & Sons, Inc., 1956.

20. Kendall, M. G. and Babington-Smith, B., "Tables of Random Sampling Numbers", Tracts for Computers, No. XXIV. London: Camb. Univ. Press, 1951.

21. Lehmer, D. H., "Mathematical Methods in Large-Scale Computing Units"; Proceedings of the Second Symposium on Large Scale Digital Computing Machinery. Cambridge: Harvard Univ. Press, 1951.

22. Hodgman, C. D., ed., "Standard Mathematical Tables". Cleveland: Chemical Rubber Publishing Co., 1931.

ACKNOWLEDGMENTS

The author wishes to express his appreciation to the numerous persons who have contributed to the success of this investigation. Many members of the faculty of the Massachusetts Institute of Technology have generously given their time and thought. Professor Ascher H. Shapiro, thesis advisor, introduced the author to this problem and has provided a great deal of valuable advice and helpful cirticism. Members of the thesis committee, Professors Holt Ashley, Edward S. Taylor, and Robert W. Mann have singly and jointly made constructive suggestions.

Edward Gugger, Dalton Baugh, and the staff of the Gas Turbine Laboratory, by freely sharing their practical knowledge and experience, provided invaluable assistance in the experimental program.

During the major portion of this investigation the author was a recipient of National Science Foundation Fellowships, enabling him to devote his full time to graduate study and research. Sponsorship by the Office of Naval Research and the use of the facilities of the M.I.T. Computation Center are gratefully acknowledged.

Finally, the author would like to express his appreciation to his parents, who unselfishly encouraged his education, to the Massachusetts Institute of Technology, which provided unparalled opportunity for this education, and to his wife, Margaret, whose patience and understanding have been largly responsible for the successful completion of this work.

BIOGRAPHICAL NOTE

The author was born in Oklahoma City, Oklahoma on October 4, 1934, and attended public schools there. He entered the University of Oklahoma in September, 1952, and the Massachusetts Institute of Technology in September, 1953. At M.I.T. he was a member of the Honors Course in mechanical engineering, Tau Beta Pi, Pi Tau Sigma and Sigma Xi. He received his S.B. degree in June, 1956.

As a recipient of a National Science Foundation Fellowship, he attended the Imperial College of Science and Technology, London, and received the Diploma of Membership of the Imperial College (D.I.C.) in July, 1957. He returned to M.I.T. in September, 1957, and was appointed Instructor in Mechanical Engineering in July, 1959.